University of Groningen

Bachelor Thesis

On the possible existence of quark stars

Author:
Leander Van Beek (S2715600)

Supervisors:
dr. ir. C. J. G. Onderwater
prof. dr. R. M. Mendez

July 17, 2018

Abstract

Neutron stars are one of the final stages after a supernova explosion before the star collapses to a black hole. They are extremely massive and have a relatively small radius. One might wonder how the transition from a neutron star to a black hole happens and whether there might be an additional stage before collapse. In this thesis the possibility of finding such a metastable star, often hypothesised as a strange star, composed of up, down, and strange quarks, is examined on the basis of the TOV-equations and by making a model for a neutron star using the polytropic equation of state. From this model, a radius-pressure relation will be derived, such that the number of baryons can be determined within a radius $r + \Delta r$ where Δr is the resolution of the simulation. Using this information, the binding energy per added baryon to the neutron star is computed. From this, we conclude that it is energetically favourable to convert the star into a strange star if a process allows this. Models of stars with Λ^0 concentrations up to 40% are also modelled, to see if they are degenerate with regular neutron stars. Observational properties of these stars are discussed.

Contents

1 Introduction

Neutron stars are astrophysical objects that spark most astronomer's imagination. They are celestial objects that have radii on the order of 10km, but comprise the mass of up to 2 $M_\odot$. Besides these extreme densities, they may also be rotating extremely fast given their proportions and have very strong magnetic fields of up to 10^8T or 10^{12} Gauss. The neutron star was theorised only in the 1930's by Fritz Zwicky and Walter Baade [1] after which the famous first observation of a pulsar was made by Jocelyn Bell: B1919+21.

The extreme densities in neutron stars make them excellent laboratories for physical processes that have not yet been able to be modelled in earth-based laboratories. This is also what is the basis of this thesis; hypothesising whether it would be possible to make a stable star from other baryons than just protons and neutrons. Protons are more stable than neutrons (the half-life of a neutron is approximately 900 seconds, while the half-life of a proton is longer than the estimated age of the universe, 14 Gyr.) but they are stable in bound form in a neutron star. A thought experiment is performed to see if nucleons containing strange quarks might also be a stable solution. Before this, an introduction to the most probable structure of neutron stars will be given.

To do this, we will use two of the equations of stellar structure: the equation of mass continuity and the equation for hydrostatic equilibrium (including their general relativistic corrections). They will be solved using the Runge-Kutta 4th order method, as they are (coupled) ordinary differential equations. Since these two equations themselves do not completely determine the behaviour of the neutron star, a polytropic equation of state is assumed. The parameters for the polytrope can be varied while finding the solutions.
With these solutions, we will then try to see if we can find configurations where the binding energy of exotic nuclei makes it energetically favourable to have a phase transition into this regime.

Firstly, we will give an introduction on some of the fundamental topics that are understood as prior knowledge during the rest of this thesis. Then, we will look into methods of storing energy inside a star to see what the effects of a transition to heavier components of the star would mean. Next, to connect this knowledge to the subject of neutron stars, we will give a brief overview of the physics involved in neutron stars. Using this chapter, we can make an estimation of the appropriateness of certain assumptions because we are familiar with the environment in which we are doing physics. Because we are partly also modelling the interactions of particles inside the neutron star, three different ways to do this through a model are discussed after which the most appropriate model is used for further analysis. To start building our simulation of the neutron star, we derive introduce the four equations of stellar structure and derive the two that are relevant for this thesis. As the two required equations are coupled, the way to solve them numerically is discussed. To give an answer to the main question, we compute the binding energies per baryon to see if it would be energetically beneficial to convert part of the baryons to hyperons. Finally observational methods that allow for detection of strange stars are discussed such that our findings can be confirmed.

2 Introduction to Fundamental Topics

In this thesis, a lot of particle physics terminology will be used. In this chapter, some important terms are briefly reviewed. A basic understanding of the standard model is assumed; the collection of the quarks in three doublets, the three pairs of leptons and the W and Z bosons as carriers for the weak force, the photon as the carrier for the electromagnetic force and the gluons for the strong force. For the comfort of the reader, some other fundamental parts of physics are briefly recapped before we dive into the physics of strange stars.

2.1 Standard Model

The framework for particle physics is called the 'Standard Model'. The standard model contains a description of the fundamental particles split up in the quarks and leptons [2]. The distinction between these particles is made by the forces that they interact with. Quarks have a colour charge, which causes them to participate in different interactions than the leptons, who do not have colour charge. The quarks are split up in three different generations, each containing two particles: the up- and down quark, the strange- and charm quark and finally the top- and bottom quark. In the leptons, such a distinction is made as well. Three generations exist, all containing a lepton and an accompanying neutrino. There is the electron with its electron neutrino, the muon and the muon neutrino and the tauon with the tauon neutrino.

The fundamental forces that all these particles interact through are mediated by the so-called *vector bosons*. Bosons and fermions are differentiated based on their spin; this is integer for bosons and half-integer for fermions. This spin reflects in differences in the behaviour of these particles, as will be shown later. Three of the four fundamental forces of nature - the strong force, the weak force and the electromagnetic force - are currently described by the standard model. Gravity still has not been unified with this theory and a unification of these theories is thoroughly sought after. The particles mediating these forces are respectively the gluons, the $W^{\pm}$ and Z bosons and the photons. Finally, the standard model contains the Higgs boson, which describes why the elementary particles (except for the photon and gluon) have masses. A visual representation of the Standard Model is given in Figure 1.

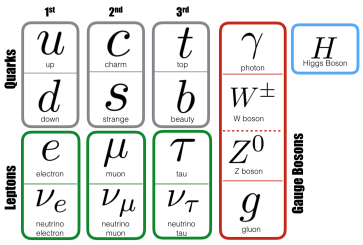

Figure 1: A visual representation of all particles contained in the Standard Model. Taken from: [3].

2.2 Fundamental Forces

Three of the fundamental forces are very relevant throughout this paper; gravity, the strong-, and weak nuclear force. Gravity is mainly involved in solving the equations of stellar structure and computing the binding energy of the particles involved in the neutron stars.

The weak interaction is at the base of the conversion process of neutron stars to exotic stars, as this is the only force that can change the quark flavour. The quark flavour is conserved for the strong interaction. It is also what makes neutron stars cool down to

their extremely low temperatures, as it is the force that mediates the Urca process [4].

$$\begin{aligned} n &\rightarrow p + e^- + \bar{\nu_e} \\ p + e^- &\rightarrow n + \nu_e \end{aligned} \tag{1}$$

Neutron stars are, however dense they may be, still transparent to these neutrinos produced by the Urca process. They carry away the energy that is left after the collapse of the supernova remnant, until most of the energy in the star is caused by the Fermi level of the constituent particles.

The strong interaction is relevant in this thesis because it is what keeps quarks confined within their nucleus. Hypotheses have been posed about deconfined quarks in the extreme pressures in the centre of a neutron star in the form of a quark gluon plasma (QGP) but we will not go into this phase in this thesis. The strong force and the way that it contains the elementary particles in a nucleon will however be discussed, as there are accessible models available that give an intuitive understanding of the confinement principle, such as the MIT bag model.

2.3 Quantum numbers

While further developing the standard model, it appeared that there were some conserved quantities throughout observed particle collisions. Initially, it was observed that during strong interactions, the neutron and proton experienced the same interaction with the strong force, despite having different charges. Other quantities of these particles are however quite similar. This pointed towards some physical symmetry causing the particles to interact equivalently; they were appointed the same new quantum number, called 'Isospin': $I_3 = 1/2$. The proton and neutron have different projections of isospin, being $+1/2$ and $-1/2$ respectively, being members of the same 'Isospin doublet'.

Isospin was one of the first 'Quantum numbers'. These numbers allows classification of particles on its fundamental properties. After Isospin, several other quantum numbers were proposed. After the 1960's, the quark model was proposed. The quark model seemed to have a nice coincidence with Isospin: the sum

$$I_3 = +1/2 * n_{up} - 1/2 * n_{down} \tag{2}$$

seemed to hold for every nucleon. Isospin was hence found to be a factor in the strong interaction between different flavours of quarks. During later particle physics experiments, it appeared to be the case that several particles, the Λ and Σ particles, were often created during experiments, but did not decay very quickly. This struck an idea for a new quark; the strange quark. As this quark is heavier than the up- and down quarks, it explained the heavier baryons. It also solved the unexpected longevity of the lifetime of these particles; the weak force interacts over much larger time scales than the strong force ($10^{-8} - 10^{-12}$s for the weak- and $< 10^{-22}$s for the strong force) [2]. During the decay of these strange particles, the number of strange quarks appeared to no longer be conserved. The new quantum number, 'Strangeness' hence appeared to be violated during the weak-, but conserved during the strong interactions.

After Isospin and Strangeness, several other quantum numbers have been proposed. These include Charm, Topness, Bottomness, Hyperspin and many more. In this thesis however, these are not mentioned and therefore we will not discuss them here.

What quantifies a good quantum number mathematically is reasonably easy. Since what we want is a proper way to describe a quantum mechanical system, a good quantum number should be an *eigenvalue* of a specified *eigenstate*, that is constant over time. Mathematically, for the Hamiltonian $\mathcal{H}$ and operator $\mathcal{O}$, q is a good quantum number for the state $|q\rangle$ if:

$$\mathcal{O}\left(q \exp\left(-iqt/\hbar\right)|q\rangle\right) = q\left(q \exp\left(-iqt/\hbar\right)|q\rangle\right) \tag{3}$$

2.4 Stability of a classical neutron star

It is reasonably well-known that a neutron in free space has a half-life of approximately 900s. Why is it that a star can be made completely of neutrons and be stable?

Several things are relevant for a neutron star. The name of a neutron star is slightly deceptive - there are still some protons and electrons around. These protons and electrons have already filled up the low-energy states that are available within the volume, such that the transition from a neutron to a proton is not very beneficially. This, and the fact that the temperatures are reasonably low (low enough to often be approximated by just the Fermi energies), makes that the decay from a neutron to a proton is not very likely. All quantum states up to the Fermi level are already occupied by the protons and electrons, with some exceptions due to the temperature not being exactly zero.

The fact that white dwarves are not collapsing is due to the degeneracy pressure of the electrons. The electrons in a white dwarf cannot be compressed any further, as the fermions just cannot occupy the same quantum volume with the same quantum numbers. This is still the case in neutron stars - the degeneracy pressure is just not sufficient. This does mean however that the electrons extend further from the centre than the neutrons do, as the neutrons are the driving force preventing collapse in this scenario. A further analysis on the pressure of fermions will be given in the following section.

2.5 The strange matter hypothesis

As mentioned before, the pressures in a neutron star may rise to such high levels that two-flavour quark states may not be the most energetically favourable position. Using the argument of the Fermi energy, it is easy to argue that a system composed of two types of quarks (p, n) has a higher Fermi energy than a system composed of particles using three quark flavors (additional particles s.a. Λ, Σ). A proposed hypothesis by Witten [5] is therefore that matter composed of just up- and down quarks is only meta-stable where matter composed of up-, down-, and strange quarks is the final ground state.

Because the Fermi momentum for a star composed of deconfined quarks is very high, a possible alternative would be the existence of exotic nucleons in the star. By weak interactions, down quarks could be converted to strange quarks. This is different from the decomposition or deconfinement of nucleons as this is manifested by the strong interaction. The interactions that keep the quarks confined within the nucleons are further treated in Chapter 7.

2.6 Energy density in a Neutron Star

To see if it is possible for regular baryons to be converted to hyperons, it is important to have an understanding of the distribution of energy throughout the neutron stars. Based on trivial arguments, one could say that the energy density is the highest in the center

of the star due to gravitational pressure, but this argument is not sufficient for making a model of the star. In this section we will first find some ballpark estimates for a probable number of baryons inside a neutron star and a binding energy per nucleon, to see if our final results are indeed sensible.

The energy density in neutron stars is very high, due to the high densities in these compact stars. With very basic tools, we can however make some crude approximations about how this energy is distributed throughout the star. For example, we can say that we can approximate the temperature in a neutron star by $T = 0$, as the Fermi momentum (10^2MeV)of the neutrons is much larger than the thermal energy (0.1MeV), which is at temperature of $T = 10^{10}$ to 10^{12}K. In the first few years of the existence of the neutron star, the star will cool rapidly by diffusion of neutrinos first and photon diffusion from the crust later, eventually reaching temperatures of 10^6K, or equivalently, 0.2keV. Sticking to this assumption limits the generality of our research, as the statements provided now cannot be applied to hot quark-gluon plasmas. How the Fermi pressure can be computed is shown in Section 6.2.

2.7 Strange matter and its formation in the universe

Strange matter is a very broad denomination for matter containing one or more strange quarks, i.e. baryons with a strange quark. Large clumps of strange matter have never been observed, but proposals for locations to find strange matter have been drafted. Two locations where this matter might be present is in so-called strangelets or, as will be investigated in this thesis, in compact neutron stars [6].

As proposed by [5], it is possible that after the big bang, some regions of the hot universe cooled down to somewhat beneath a temperature T_c required for a first order phase transition. These would have formed 'bubbles' of condensed baryonic matter that expanded and eventually dominated the universe. The hotter regions of the universe would become more and more compressed, as losing the latent energy takes more time than the expansion of the universe, assuming that the most of the energy loss is due to neutrinos escaping these regions (which is a hopeful assumption). These hot regions would eventually take the form of bubbles in the universe and could still be around, containing strange matter. The abundance of these bubbles in the Milky Way is somewhere in the range of $5 \times 10^{-34} - 5 \times 10^{-43}\text{cm}^{-3}$ and they have velocities of the order of $2 \times 10^7\text{cm}\,\text{s}^{-1}$. This comes down to a flux of $10^{-26} - 10^{-35}\text{cm}^{-2}\,\text{s}^{-1}$. The abundance of neutron stars in the Milky Way is approximately $\frac{10^9}{6\times10^{66}\text{cm}^3} \approx 2\times10^{-58}\text{cm}^{-3}$. With an average radius of 10km, this gives a total collision area of $\pi * (10^5)^2 \times 10^9 = 3 \times 10^{19}\text{cm}^2$. The collision rate of the hot quark bubbles with neutron stars is thus approximately $3 \times 10^{-7}\text{s}^{-1}$, or one every year. It is also hypothesized that stars that already contain strange matter, can produce strangelets by colliding with other objects (say, a binary companion). They can expel some of the strange matter upon colliding.

As previously mentioned, strange matter is also hypothesised to form in compact stars. As the strange baryons is heavier than the proton and the neutron, it is able to store more energy as binding energy and therefore being more stable. The energy that is stored while transitioning from regular nucleons to strange baryons not only stores energy in the form of binding energy, it also allows for compactification of the star as strange baryons possess different quantum numbers than protons and neutrons and therefore experience no Pauli pressure due to these particles.

Finally, a theory by Boden is that regular matter might only be a meta-stable state,

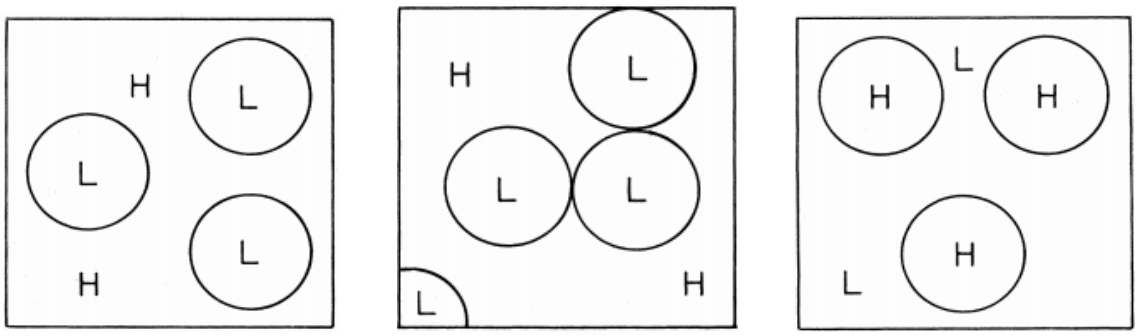

(a) Low-temperature bubbles are isolated

(b) The low-temperature bubbles expand and meet

(c) The high-temperature medium is now isolated

Figure 2: Expansion of low-temperature bubbles in the early universe. *Taken from: [5]*

that can still decay to strange matter. This argument is also based on the principle of Pauli pressure, as with an additional quantum number, you can place more quarks in lower-energy states than with only two quantum numbers. The simple strange baryons decay because the fact that they are only with small amounts in a nucleon, such that enough low-energy states are available, where exotic baryons that contain more quarks would not have this disadvantage.

3 Storing the energy

3.1 Gravitational potential energy

There is a very simple way to store energy in the form of binding energy. When we have two separate masses in a volume, they interact through the gravitational force. As is trivial, they will accelerate towards their common centre of mass. If two objects are gravitationally bound and placed close together, one needs a force to take them apart again. The work that is performed by separating these masses from distance zero to infinity is the path integral of the force: this is the gravitational binding energy. It is the same as the gravitational potential

$$U = -\frac{GMm}{r} \tag{4}$$

Due to the mass-energy equivalence principle we can convert this binding energy to an added mass through the famous (non-relativistic) equation of $E = mc^2$. When you try to take the two masses apart, you have to add energy - and hence mass. The effective mass of the masses is therefore related through

$$m^* = m_0 + \frac{E_{bind}}{c^2} \tag{5}$$

Bound masses (it can be macroscopic masses as well as nuclei) are therefore lighter when they are bound together than the sum of their constituents. Macroscopic masses are bound by different interactions than nuclei however, as gravity does not act significantly on this scale.

3.2 Liquid Drop Model

Binding energy is stored in the nuclei due to the strong nuclear force. The nucleus can be modelled similar to a liquid droplet. The liquid drop model, giving rise to the semi-empirical mass formula, is as follows. [7]

$$\begin{aligned} M(Z,A) = Z(m_p + m_e) + (Z-A)m_n - a_1 A + a_2 A^{2/3} + a_3 \frac{Z(Z-1)}{A^{1/3}} \\ + a_4 \frac{(Z - A/2)^{1/2}}{A} + a_5 A^{-1/2} \end{aligned} \tag{6}$$

All terms are based on some proportionality to the atomic or charge number of the nuclear. The first two terms are just the sum of the mass of the constituents.
The third term, confusingly often labelled a_1 is the volume correction term, which has a negative contribution because of the range of the strong force. The diameter of a proton is approximately one femtometer, so for heavier nuclei the diameter of the nucleus can be several femtometers. As the range of the strong force is only approximately on the order of one femtometer, not all nuclei are bound by the strong interaction with all other particles.
The fourth term (a_2) is the surface area term; this scales with the radius of the nucleus to the two-third, which is proportional to surface area. ($R^3 \propto M \propto A \Rightarrow A^{2/3} \propto R^2 \propto S$, S the surface of a spheroid). Just as for a liquid drop, the surface tension keeps the droplet together. The entities on the inside are omnidirectionally attracted to their neighbours and there is no net intermolecular force. For the entities on the surface, the bonds that bind the droplet together are much stronger than those towards the outside interface. The entities are hence more packed together in this area and hence there is a higher energy density. This is why this has a positive contribution to the binding energy.

The fifth therm (a_3) is due to the Coulomb interaction between the protons - one expects the proportionality $Z(Z-1)$ in this term. As the forces between the protons are repulsive, this decreases the net mass.
The sixth term (a_4) is called the antisymmetry term or the Pauli term. From the chart of stable nuclei, we see that the ratio of neutrons to protons in stable nuclei tends to right, i.e. there are more neutrons then protons.
The final term, labelled a_5, is the pairing term. The pairing term exists because of Hund's

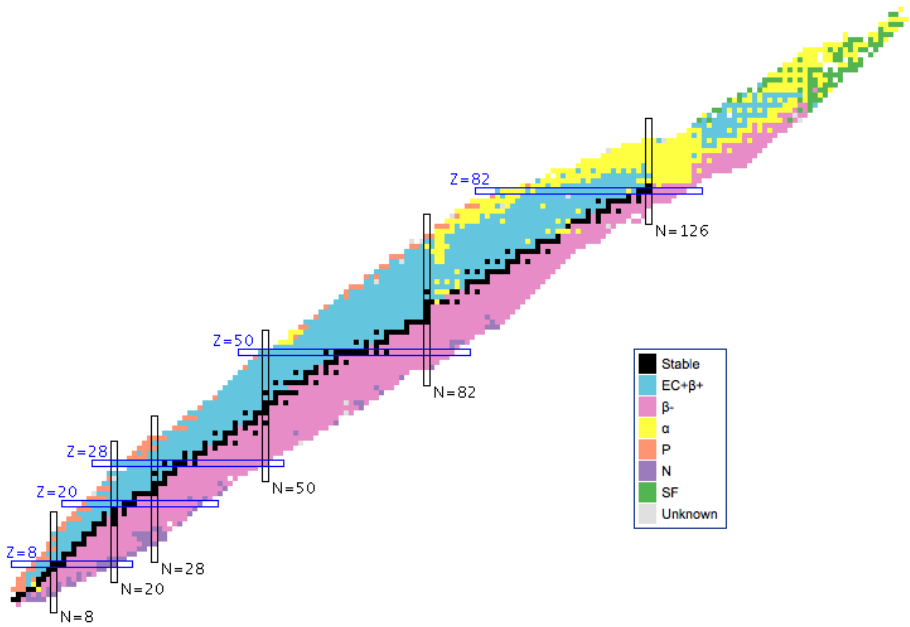

Figure 3: Isotope chart. The ratio of protons to neutrons starts to decrease for larger amount of protons. *Taken from: paketsusudomba.co*

rules for nuclei. From principles of statistical physics it follows that the configuration with the highest degeneracy is energetically favourable. When the nucleus can be configured with an even number of protons and neutrons, these can be configured in a net spin-0 configuration, which is energetically most favourable. When the protons or neutrons are present an odd number of times, this term adds a certain amount to the mass of the nucleus:

$$a_5 = \begin{cases} a_5(>0), & \text{if Z odd} \\ 0, & \text{if Z even, A-Z odd} \\ -a_5(<0), & \text{if Z even, A-Z even} \end{cases} \tag{7}$$

We will use the liquid drop model for a justification of the structure of the outer neutron crust. Here, we will first apply it to a whole neutron star to get an order of magnitude estimate for the amount of binding energy involved in a neutron star. An average neutron star has a mass of two solar masses, i.e. $2 \cdot 2 \times 10^{30} kg$. Divided by a nuclear mass, this gives us a baryon number on the order of $B = 10^{56}$.

The first thing we notice is that the term containing a_3 in Equation 6 goes to zero as the number of neutrons is much larger than the number of neutrons in a neutron star. The second thing we see is that the term containing the coefficient a_5 is also negligible, as $(10^{56})^{-1/2} = 10^{-28}$. Finally, we notice that the binding energy is the mass of the constituents substracted by the mass according to this model, such that we substract the terms for the proton, electron, and neutron masses. Using the fitted parameters $a_1 = 15.76$MeV, $a_2 = 17.81$MeV, $a_3 = 23.702$MeV [8], we find a binding energy on the

order of

$$\begin{aligned} E_b &= -15.76\text{MeV} \times 10^{56} + 17.81\text{MeV} \times \left(10^{56}\right)^{2/3} + 23.702\text{MeV} \times \frac{\left(-10^{56}\right)^2}{10^{56}} \\ &= -9.834 \times 10^{56}\text{MeV} = -9.834\text{MeV} \times B \end{aligned} \tag{8}$$

where the binding energy is negative because it needs to be *added* to the system to take it apart.

3.3 What happens to this enormous energy?

The approximate 10^{57}MeV that came out of the order of magnitude estimate of the previous chapter can be increased even further. This approach will use only the gravitational binding energy approach, as the liquid drop model starts to fail here.
In Equation 4, we see that the binding energy increases further when we replace a neutron with mass $m_n = 939.565\text{MeV}\, c^{-2}$ for a particle with a larger mass. Take for example the Λ^0 baryon, with a mass of $m_{\Lambda^0} = 1115.683\text{MeV}\, c^{-2}$. By converting available energy in the system equivalent to the mass difference of the two baryons to mass, we increase the binding energy (i.e. we make the binding energy *more negative*). To give a comparison with the gravitational binding energy of a nucleon; we will find from our models that the gravitational binding energy per nucleon can be up to 80MeV for certain models.

The stability of a system is often characterised by the depth of its potential well. One might hence naively say that a neutron star including Λ^0 particles is hence more stable then a pure neutron star. There is however one problem; the Λ^0 boson is composed of an up, down and strange quark. Converting a neutron, composed of an up, down, and down quark to a Λ^0 boson is not often done naturally. So how does this happen? This question will be touched on in a later chapter. From here on we are assuming that this process is *just happening*, and not interfering with the rest of the physical system.

When adding new baryons to the system, we open up another possibility besides increasing the binding energy. As is theoretically modelled, the neutron star is held up by neutron degeneracy pressure. This degeneracy pressure is an effect of the Pauli exclusion principle which states that no two fermions with the same quantum number can occupy the same quantum volume. But since Λ^0 particles have different quantum numbers than neutrons, they are not affected by their Fermi sea! The star can hence be compressed into a smaller volume. There is a final limit however; once the star collapses within a radius called the Schwarzschild radius, the star collapses into a black hole.

$$R_S = \frac{2GM}{c^2} \tag{9}$$

which is approximately 3km per solar mass.
It is well-established that the major properties of the star are almost completely determined by its mass and radius. Under this thought experiment, exactly these two parameters change by a significant amount. In the rest of this thesis, we will continue to look into the consequences this has for a neutron star. Firstly however, we will give a small introduction to the basics of a neutron star.

4 Introduction to Neutron Stars

Neutron stars are relatively unknown objects, although we know of the existence of several hundreds of neutron stars (about 2000 in 2010). The intrinsic physics of the neutron stars is a difficult topic as the formation of these stars is understood in the big picture, but the specifics are often based on assumptions of the involved stellar composition.

Neutron stars were first discovered by Jocelyn Bell, at the time still a student at Cambridge, while going through observational data that was obtained to find sources with rapidly varying fluxes in the radio regime (wavelengths of 1cm to 30m). She found a rapidly fluctuating flux at a very regular rate. What she had found was in fact a pulsar; a rapidly rotating neutron star [9].

4.1 Origin

When a star with a mass of more than approximately 8 $M_\odot$ has burnt all its 'advantageous' fuel, it can no longer produce energy in the core by fusion. Up to this point, the binding energy of higher elements was larger than that of current elements, allowing the star to produce energy to prevent its collapse. The binding energy per nucleon in a specific nucleus has its peak around Fe-56, as can be seen in Figure 4. The radiation pressure generated in the core of the star due to these fusion processes is no longer enough to balance the gravitational pressure and the star starts to collapse. During the collapse, the other shells of the stars continue to fuse their materials [10].

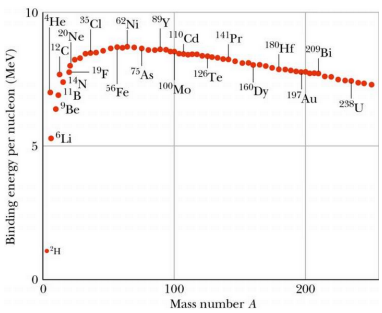

Figure 4: Binding energy per nucleon in MeV, Taken from: `physics.ohio-state.edu`

Firstly, the electron degeneracy pressure starts to rise. This effect is due to filling the phase space by blocking of the Pauli exclusion principle for electrons. For proto-neutron stars, this pressure is however not high enough to prevent further collapse from stellar remnants with masses of over 1.44 $M_\odot$(The Chandresekhar Mass [11]). Due to the high temperatures and thus high energies that are available in the star in the form of the chemical potential of the electrons, the iron nuclei are starting to decompose and electron capture starts to manifest itself. The reaction $e^- + p \rightarrow \nu_e + n$ releases a lot of energetic neutrino's - with this mechanism, the star is able to rapidly cool from temperatures of 10^{11}K to temperature around 10^6K. This process of cooling through neutrino emission is also known under the name 'Urca process' [4].
All the newly formed neutrons also partake in the fermionic distribution of states in the stellar core and this starts to realise a significant pressure that finally halts the collapse of the star. There is now a very rigid sphere with central densities of up to several $10^{17}\mathrm{kg\,m^{-3}}$ or $10^{14}\mathrm{g\,cm^{-3}}$.

This brief overview, that only stops at neutrons in the core, is only a simple model of neutron stars; there are several hypotheses about further decomposition processes in neutron stars. This will be treated in the section on the structure of neutron stars, Section 5.

4.2 Pulsars

Pulsars were the first forms of neutron stars to be discovered. When a star collapses, its radius obviously decreases. The mass lost due to e.g. neutrino cooling is not very significant, such that due to conservation of angular momentum, the star has to speed up its rotation. The magnetic field of the star is also contained in a smaller volume, making for a stronger field. From Maxwell's third equation, $\nabla \times E = -\frac{\partial B}{\partial t}$, we know that an electric field is generated in this situation. This electric field is what Jocelyn Bell in fact observed when she observed the first neutron star.

5 The structure of Neutron Stars

The process in neutron stars is not as simple such that it stops at forming a solid sphere of neutrons. From the surface of the star, which conceptually is quite easy, we will go deeper down the core of the star.

5.1 The Crust of a Neutron Star

The crust of the neutron star is most likely made up of left over ions and iron atoms, together with some separate protons and neutrons. In this region, the pressure is not high enough to continue the electron capture process. Simply by subtracting the masses of a proton and an electron from a neutron, one sees that at least an additional 780keV is required, which corresponds to a temperature of almost 10^{10}K.

$$m_n - m_p - m_e = 780\text{keV}/c^2 \Rightarrow T = 780\text{keV}/c^2/k_b = 9.1 \times 10^9\text{K} \tag{10}$$

It is possible to have the outer crust of the neutron star made up of Fe-56 nuclei, as the binding energy of this nucleus is 8.8MeV per nuclei - corresponding to temperatures of 10^{11}K.

The outer crust of the neutron star is approximately 500m wide. [12] Beyond this layer, we have densities of $\rho_{drip} = 10^{14}\text{kg}\,\text{m}^{-3}$, which is the densities at which neutrons start to drip from nuclei. The range of the strong force is no longer sufficient to keep all the nuclei bound together. This process is what makes the ratio of neutrons over protons in a neutron star so high; we are on the right side of the band of stability of Figure 3. The electron capture makes the amount of neutrons in a nucleus so high that we end up on the right side of the band in stability in Figure 3. The number density of neutrons increases until we reach the end of the inner crust at $n_0 = 0.16\text{fm}^{-1}$; we have reached the inner structure of the star at a depth of approximately 1km.

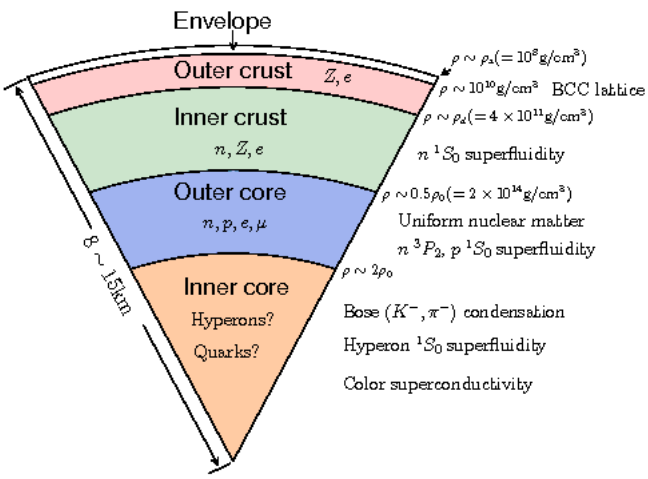

Figure 5: Schematic overview of the regions in a neutron star. Taken from: inspirehep.net

5.2 Going deeper in a neutron star

The structure from the crystalline structure that occurs at densities around the nuclear density makes room for a new phase of matter; the quark gluon plasma. Just as a normal plasma, where the components of a normal atom are split up in its nucleus and free roaming electrons [13], the constituents of the nuclei are now split up as well. The quarks that

make up the nucleons roam around 'outside' the volume of the nucleon - although now a clear distinction of a 'nucleon' can no longer be made. At this point, the 'whiteness' of individual particles is also no longer guaranteed as quarks themselves carry colour charge. The interactions in this phase of matter are mainly due to the strong interactions between the quarks, mediated by the gluons.

Before the crystalline structure transfers to the plasma however, several interesting phase transitions are proposed. The QGP will be discussed here for the sake of completeness on the description of neutron stars. During the later modelling of the neutron stars, the QGP will not be taken into account. More on this can be found in the respective chapters.

The phase transitions from the inner crust to the core happens in so-called "pasta phases". The name of these phases comes from the similar geometrical appearance to several pasta shapes. [14] Why this happens is based on a simple argument between the magnitudes of the Coulomb interaction and the surface tension of the nucleus. Let us make an order of magnitude estimate based on the energy of these interactions taken from the Liquid Drop Model [7]. Remember that we had the binding energy of a nucleus given by Equation 8:

$$E_B = a_V A - a_s A^{2/3} - a_c \frac{Z^2 e^2}{A^{1/3}} - a_A \frac{(A-2Z)^2}{2A} + \delta(A,Z) \tag{11}$$

We will be focussing on the second and third term on the right hand side of the equation. The Coulomb energy is given by $E_{coul} = \frac{3}{5} Z^2 e^2 r_n$, where the radius of the nucleus $r_n = A^{1/3} R_0$. The surface energy is given by $E_{surf} = a_s A^{2/3}$. The binding energy per nucleon for both terms is then proportional to $E_{coul}/A = \frac{3}{5}\frac{Z^2 e^2}{A^{4/3}} \propto A^{-4/3}$, where for a constant ratio Z/A, we find $E_{coul}/A \propto A^{2/3}$ for the Coulomb term. For the surface energy this is $E_{surf}/A \propto A^{-1/3}$. Finding the minimal energy while leaving the other terms invariant can then be done through

$$\begin{aligned} 0 &= \frac{\partial}{\partial A}\left(\frac{E_{coul}}{A} + \frac{E_{surf}}{A}\right) \\ &\propto \frac{\partial}{\partial A}\left(A^{2/3} + A^{-1/3}\right) \\ &= \frac{2}{3}A^{-1/3} - \frac{1}{3}A^{-4/3} \\ &\Rightarrow 2E_{surf} = E_{coul} \end{aligned} \tag{12}$$

such that we see that the Coulomb forces dominate when the energy is larger than twice the surface tension, $E_{coul} \geq 2E_{surf}$. The Coulomb force deforms the nucleus and is now no longer counteracted sufficiently by the surface tension of the nucleus. Spherical nuclei are now no longer the most beneficial packing form, and the nuclei start to bind together in spheres (also called the gnocci phase). If the density becomes higher, the spheres begin to form rods (spaghetti phase) and later sheets (lasagna phase). After this phase, the clustered neutrons are the more common phase of matter and the 'anti-pasta phases' set in. The unclustered neutrons form the same geometrical shapes as the clustered neutrons did before, in opposite order. For a visualisation, see Figure 6.

The density gets even higher when we continue to the central core of the neutron star. Here, the density is at least equal to the density ρ_0 (Equation 13) of 0.122fm^{-3} or $2.04 \times 10^{14}\text{kg}\,\text{m}^{-3}$. At these densities, the 'confinement bags' of the nuclei start to interact using the strong interactions. What happens exactly in this phase is treated in

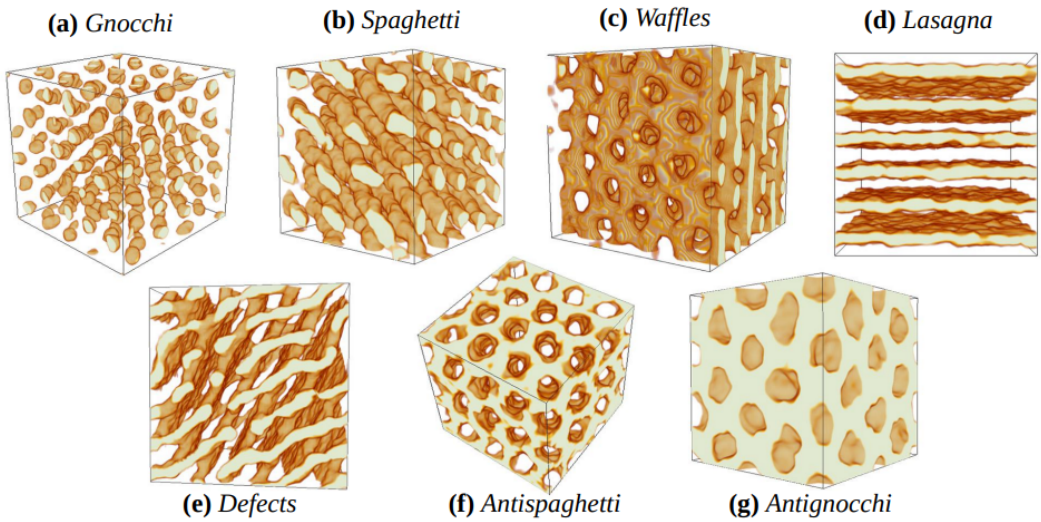

Figure 6: Visualisation of the simulations on the 'Pasta phases' in the inner core of a neutron star. Taken from [15]

the following chapters.

$$n = \frac{A}{\frac{4}{3}\pi R^3} = \frac{A}{\frac{4}{3}\pi (A^{1/3} R_0)^3} = \frac{3}{4\pi (1.25\text{fm})^3} = 0.122\text{fm}^{-3} \tag{13}$$

6 Interactions of Particles

As mentioned in the previous chapters, there are several fundamental forces of nature. These modelling of these forces is very complex and can generate very large simulations. Because this is only a bachelor project, we will assume simpler models for the interactions between these particles. These models consist of a previously worked-out equation of state, considering for example the sphere size of nuclei, the interactions between them and their quantum mechanical behaviour. Several equations of state can be considered, but throughout this thesis we have made approximations based on the 'hard sphere model', the Fermi model for an fermion gas, the Van der Waals equation for a real gas and the polytropic equation of state. Below, we will expand on these models.

6.1 Hard Sphere Model

The hard sphere model is, superficially, the most simple of the models. The hard sphere models consider all the nuclei as massive spheres with a certain radius and charge (say, $1e$ for a proton) after which you can put these spheres together to form a nucleus or a baryonic gas.
The difficulty in this model lies in the fact that approximating a radius for a proton or a neutron is not trivial in any way. One could ask himself the question what the mass-radius or charge-radius relation is for a proton. To answer these questions, research has done that came up with the concept of the form factor. The form factor can be determined experimentally, and is related to the radius of the nucleus that you are scattering against. If an electron is scattered against a nucleus, it is deflected towards some solid angle $d\Omega$ with a probability of $\frac{d\sigma}{d\Omega}$. This probability is affected by the potential and hence interaction with the nucleus, contained in the term M_{fi} and the density of final states D_f. These are all related through

$$\frac{d\sigma}{d\Omega} = \frac{2\pi}{\hbar} \left|M_{fi}\right|^2 D_f \tag{14}$$

As was said, M_{fi} models the interaction through the potential of the nucleus. This is done through

$$M_{fi} = \int \psi_f^* V(\vec{r}) \psi_i d^3r \tag{15}$$

The potential experienced by the electron at a distance $\vec{r}$ from the nucleus is just the Coulomb potential. Applying this, and making the plane wave function assumption for ψ, one finds for M:

$$M_{fi} = -\frac{Ze^2}{4\pi\epsilon_0} \int\int e^{i(p_f - p_i)\cdot\vec{r}/\hbar} \frac{\rho(r')}{|r - r'|} d^3r' d^3r \tag{16}$$

At this moment we can make the distinction between a point-like nucleus or a finite-volume nucleus. In the first case, the charge is considered to be entirely enclosed in a singular point. The charge density is then a delta function, and the result that is obtained is that of Rutherford scattering. When we assume a finite volume, the term $\int e^{iq\cdot\vec{r}/\hbar}\rho(r)d^3r$, $q = p_f - p_i$ is then known as the form factor, dubbed $F(q)$. Now as most of the terms in this equation are known, it is possible to determine the charge density $\frac{d\sigma}{d\Omega}$ through scattering experiments, as this is just the distribution of the electrons after the scattering experiment. From this, the form factor $F(q)$ can be determined. To obtain $\rho(r)$ is then quite simple, as it is quickly seen that this is just the Fourier transform of the form factor. Using such scattering experiments, the radius of the proton has been determined to be $r_p = 0.8751 \pm 61$fm [16]. This value will hence also be assumed when we try to model a system using the hard-sphere model.

The first model for a strange star will be made using this simple concept, but it will prove insufficient.

6.2 Fermi gas

The fundamentals of a Fermi gas are important in this thesis for several reasons. For one, there is the assumption of zero temperature in a Neutron star. This is based on the Fermi gas. Also, as the densities in a neutron star are sufficiently high and the temperatures sufficiently low, the distribution of the energy states for the Fermions (as well neutrons as protons as electrons as Λ^0) is based on this distribution. This is a motivation to work through the derivation of a Fermi gas; both to show that the zero temperature approximation holds, as well as getting an intuition for the distributions involved.
To show where the Fermi pressure comes from, we will derive it from some first principles of statistical physics. In this case, the derivation for the Fermi pressure will be done for the electrons, but it can be done similarly for other fermions such as neutrons.
We know from statistical physics [17] that the density of states is given through

$$f(k)dk = g\frac{4\pi k^2}{(2\pi\hbar)^3}dk \tag{17}$$

where g is the degeneracy - two for the spin, in our case. From this, as the distribution function $f = \frac{dn}{dk}$, we can obtain

$$dn = 2 * \frac{4\pi k^2 dk}{(2\pi\hbar)^3} = \frac{k^2}{\pi^2\hbar^3}dk \tag{18}$$

We can rewrite this for the electron density, integrating from no momentum to the fermi momentum.

$$n_e = \int_0^{k_F} \frac{k^2}{\pi^2\hbar^3}dk = \frac{1}{3\pi^2\hbar^3}k_F^3 \tag{19}$$

It is possible to find another expression for the electron density as well. We know that in a star that is approximatly neutral, the electron density can be written as

$$n_e = \frac{\bar{\rho}}{m_n}\frac{Z}{A} \tag{20}$$

As most of the mass of the star comes from the mass of nucleons, we can say that $\rho \approx \epsilon/c^2$, where ϵ is the energy density. The energy density of the electrons is the sum of their rest masses and their kinetic energy, giving as a result

$$\epsilon_e = \frac{1}{\pi^2\hbar^3}\int_0^{k_F}\left(k^2c^2 + m_e^2c^4\right)^{1/2}k^2dk = \frac{1}{\pi^2\hbar^3}\int_0^{k_F}E(k)n(k)dk \tag{21}$$

Integrating this, we come up with the following expression for electron energy density

$$\begin{aligned}\epsilon_e(k_F) &= \frac{m_e^4c^5}{\pi^2\hbar^3}\frac{1}{8}\left[\left(2\left(\frac{k_F}{m_ec}\right)^3 + \frac{k_F}{m_ec}\right)\left(1+\left(\frac{k_F}{m_ec}\right)^2\right)^{1/2} - \operatorname{arcsinh}\left(\frac{k_F}{m_ec}\right)\right] \\ &= \epsilon_0\left[\left(2\left(\frac{k_F}{m_ec}\right)^3 + \frac{k_F}{m_ec}\right)\left(1+\left(\frac{k_F}{m_ec}\right)^2\right)^{1/2} - \operatorname{arcsinh}\left(\frac{k_F}{m_ec}\right)\right]\end{aligned} \tag{22}$$

Due to the low temperature of neutron stars and white dwarfs, the momentum of nucleons is not considered in the energy contribution. Only the momentum from the electrons is

considered. When we set the masses of protons and neutrons equal, as $\frac{m_n}{m_p} \approx 0.999$, the result is

$$\epsilon = m_n * n_e * \frac{A}{Z}c^2 + \epsilon_e(k_F) \tag{23}$$

With a simple argument and a not so simple integral, we can relate the energy density to the pressure. Assuming the distribution of momentum in the star is isotropic, all momentum is equally divided over all solid angles. As a particle scatters, its transferred momentum is proportional to its angle of incidence through $\cos\theta$, θ the angle of incidence, and the fraction of the radiation pointed at each solid angle is also proportional to $\cos\theta$. As a sphere spans 4π solid angles and a solid angle $d\Omega$ is defined as $d\Omega = \sin\theta d\theta$, we integrate and find a factor of 1/3.

$$\frac{1}{4\pi}\int_0^{2\pi} d\phi \int_0^{\pi} \cos^2\theta \sin\theta d\theta = \frac{1}{2}\left[-\frac{1}{3}cos^3\theta\Big|_0^{\pi}\right] = \frac{1}{3} \tag{24}$$

Hence we know the pressure to be

$$\begin{aligned} P &= \int_0^{k_F} \frac{1}{3}\epsilon(k)dk \\ &= \frac{1}{3}\epsilon_0 \left[\left(2\left(\frac{k_F}{m_e c}\right)^3 - 3\left(\frac{k_F}{m_e c}\right)\right)\left(1+\left(\frac{k_F}{m_e c}\right)^2\right)^{1/2} + 3\sinh^1\left(\left(\frac{k_F}{m_e c}\right)\right)\right] \end{aligned} \tag{25}$$

So far we have neglected the contribution of kinetic energy of nucleons, since these are a factor $\sqrt{10^9}$ smaller than the rest mass energy at temperatures of neutron stars (a few thousand Kelvin).
Now the result above is analytical. It is possible to work from Equation 25 and obtain a more useful equation that we can use in the analysis for a polytropic equation of state. It is at this moment that we can make a distinction between the relativistic ($k_F \gg m_e c$)and non-relativistic system ($k_F \ll m_e c$). Returning to one of the intermediate steps of Equation 25, temporarily substituting $x = \frac{k_F}{m_e c}$, and going into the non-relativistic domain where x is hence small:

$$p_e(k_F) = \frac{\epsilon_0}{3}\int_0^{k_F} \frac{x^4}{\sqrt{x^2+1}}dx \approx \frac{\epsilon_0}{3}\frac{x^5}{5}\Big|_0^{k_F} = \frac{\epsilon_0 k_F^5}{15(m_e c)^5} \tag{26}$$

using the identity 18, we find $k_F = \sqrt[3]{\frac{3\pi^2\hbar^3\rho Z}{Am_n}}$ this to

$$p_e(k_F) = \frac{m_e^4 c^5}{\pi^2\hbar^3}\frac{1}{15}\frac{\hbar^5}{(m_e c)^5}\sqrt[3]{\frac{3\pi^2\rho Z}{Am_n}} \tag{27}$$

and we have found the pressure of a pure electron Fermi gas. Using this equation for the pressure, we can show that the temperature inside the neutron stars are negligible.

6.3 Van der Waals gas

The Van der Waals gas is a model for gasses that is more likely to provide correct results for real gasses than the equation of state for a perfect gas. The perfect-gas assumptions are among others that the particles in the gas are point-like, do not interact (i.e. they do not repel or attract each other at any radii) and they only partake in elastic collisions. This is of course not the case in a neutron star, but it gives a better approximation than the hard-sphere model, as this both crashes our simulation and gives unphysical solutions. The perfect gas can be derived from just assumptions in statistical physics. As the probability of a particle being in an energy state E_r is proportional to $p(E_r) \propto -\exp(-\beta E_r)$,

where $\beta = (kT)^{-1}$. The partition function then normalises all the probabilities for all these energy states, through

$$p(E_r) = \exp(-\beta E_r)/\Sigma_i \exp(-\beta E_r) \tag{28}$$

This would result in the probability distribution for a single-particle state. For a multi-particle state, we cannot just raise the partition to the power of the number of particles, as then we would be counting some states twice, weighing them wrong. We actually get

$$Z = \frac{1}{N!}\left[\Sigma_r \exp(-\beta E_r)\right] \tag{29}$$

Now we should note that the energy of the system is the sum of all internal energy states and the sum of all translational eigenstates. For the translational energy distribution, we assume that $E_r = \frac{p_r^2}{2m}$. Now the density of states for a particle with its momentum $p \leq p_r \leq p + dp$ and its energy between $E \leq E_r \leq E + dE$ is given by

$$f(p)dp = \frac{V 4\pi p^2 dp}{h^3} \tag{30}$$

As Z can give the integral probability normalisation factor of all particle states, we can see

$$Z = \int_0^\infty \frac{V 4\pi p^2 dp}{h^3} \exp\left(-\beta \frac{p^2}{2m}\right) = V\left(\frac{2\pi m k_b T}{h^2}\right)^{3/2} \tag{31}$$

Now remember that we added a factor of $\frac{1}{N!}$ to assure correct weighing of states and a power N for the number of particles, the multi-particle translational partition function is

$$Z = \frac{1}{N!} V^N \left(\frac{2\pi m k_b T}{h^2}\right)^{3N/2} \tag{32}$$

At this stage, we can already express some useful thermodynamic quantities, e.g. the Helmholtz free energy. Making use of an identity called Stirling's approximation: $N! = \left(\frac{N}{e}\right)^N$, we have for the Helmholtz free energy:

$$A = -k_b T \ln(Z) = -N k_b T \ln\left(\frac{eV}{N}\left(\frac{2\pi m k_b T}{h^2}\right)^{3/2}\right) \tag{33}$$

The equation so far only holds for a gas where the average occupancy of a state is low, that is, $n_r \ll 1$. As the probability for a state was $\frac{\exp(-\beta E_r)}{Z}$ and $\bar{n_s} = N\text{prob}(E_s)$, we find the inequality

$$\bar{n_s} = \left(\frac{N}{V}\left[\frac{h^2}{2\pi m k_b T}\right]^{3/2}\right)\exp(-\beta E_r) \ll 1 \Rightarrow \frac{N}{V}\left(\frac{h^2}{2\pi m k_b T}\right)^{3/2} \tag{34}$$

From this inequality, the boundaries of this simple model for a gas become clear. For the inequality to hold, you could have either very large volumes V or very large temperatures T. Large temperatures here are of course on the Kelvin scale, such that this model can be applied in the ordinary situations around us.
Finally, the equation for a perfect gas can be obtained from

$$P = -\left(\frac{\partial A}{\partial V}\right)_{T,N} = -\left(-N k_b T \frac{1}{V}\right) \Rightarrow PV = N k_b T \tag{35}$$

This can also nicely be connected to the De Broglie wavelength. The De Broglie wavelength is given by

$$\lambda_{dB} = \frac{h}{p} = \frac{h}{\sqrt{2mE_r}} = \frac{h}{2m3/2k_b T} \Rightarrow \frac{h}{\sqrt{3mk_b T}}\sqrt{\frac{3}{2\pi}} \tag{36}$$

$$\sqrt{\frac{3}{2\pi}}\lambda_{dB} = \sqrt{\frac{h^2}{2\pi m k_b T}} \tag{37}$$

$$\left(\frac{N}{V}\right)^{1/3}\sqrt{\frac{3}{2\pi}}\lambda_{dB} = \left(\frac{N}{V}\right)^{1/3}\sqrt{\frac{h^2}{2\pi m k_b T}} \ll 1 \tag{38}$$

Now we know that $(N/V)^{1/3} = l$, basically the interparticle separation.

$$\sqrt{\frac{h^2}{2\pi m k_b T}} = \sqrt{\frac{3}{s\pi}}\lambda_{dB} \ll l \tag{39}$$

Now assuming the term in the square root on the right hand side to be approximately one, this gives the conclusion

$$\lambda_{dB} \ll l \tag{40}$$

The de Broglie wavelength has to be much smaller than the interparticle separation to have the perfect gas equation to hold! This is also in agreement with the two requirements that we mentioned before.

Now to have interaction also play a role in the equations, we make the partition function a bit more complicated.

$$Z = \frac{1}{N!}\left(\int \frac{d^3\vec{r}d^3\vec{p}}{h^3}\exp\left(-\frac{\beta\vec{p}}{2m}\right)\right)^N = \frac{1}{N!}\int \frac{1}{h^{3N}}d^3\vec{r_1}\dots d^3\vec{r_N}d^3\vec{p_1}\dots d^3\vec{p_N}e^{-\beta K} \tag{41}$$

Where K is the sum of all the momenta of the states in the system squared, divided by $2m$ - the kinetic energy of the gas. To switch on interactions, we change the K for an H. The H is composed as $H = K + U$ where U represents interactions between different particles in the gas. As the addition in the exponent can just be seen as a multiplication of twice as many radius- and momentum terms, we know get

$$Z_{interactions} = Z \times \left[\frac{1}{V^N}\int d^3r\vec{r_1}\dots d^3\vec{r_N}\exp\left(-\beta U\right)\right] = Z \times Q \tag{42}$$

Now we have to make another approximation here to keep things manageable. The potentials are all dependent on the distance between the particles, and the particles of course experience more interactions than one at the same time. This would cause a term of $\Pi_k(\exp(-\beta a_k))$ for all the interactions between all the particles. As we can impossibly model all these interactions simultaneously, we will choose to take only the two-particle interactions. Leaving aside the mathematical rigour - a clever trick in describing the interactions mathematically [17]- we end up with the expression

$$Q = \frac{1}{V^N}\int d^3r\vec{r_1}\dots d^3\vec{r_N}\left[1 + \sum_{i,j,i\neq j}\lambda_{ij}\right] \tag{43}$$

$$\frac{1}{V^{N-2}}\int d^3\vec{r_1}d^3\vec{r_2}\left[\lambda_{12}\right]\frac{N(N-1)}{2} = \frac{N^2}{2V^2}\int d^3\vec{R}d^3\vec{r}[\exp(-\beta u(r)) - 1] = \frac{N^2}{2V}I_2 \tag{44}$$

Finally, this means for Q:

$$Q = \left(1 + \frac{N^2}{2V}I_2 + \dots\right) \tag{45}$$

Where ... represent here the higher-order interactions. Now there's only two more steps towards the expression for the pressure of a Van der Waals gas. First, as for the perfect gas, we compute the Helmholtz free energy.

$$A = -k_bT\ln(Z) = -k_bT\ln(Z\times Q) = A_p + k_bT\ln\left(\left(1+\frac{N}{2V}I_2\right)^2\right) \approx A_p - k_bT\frac{N^2}{2V}I_2 \tag{46}$$

Now to obtain the pressure, we take again the partial derivative with respect to the volume.

$$P = -\left(\frac{\partial A}{\partial V}\right)_{T,N} = -\left(\frac{\partial}{\partial V}\left[A_p - \frac{kTN^2}{2V}I_2\right]\right)_{T,N} = \frac{Nk_bT}{V}\frac{k_bTN^2}{V^2}I_2 \tag{47}$$

Now this part is were it becomes interesting, as I_2 is the interaction strength between two particles. It is possible to fill in any arbitrary potential here, but often a potential like Figure 7 or equation 48 is chosen.

$$-\lambda(\vec{r}) = \begin{cases} 1 & \text{if } 0 < \vec{r} < 2r_0 \\ \frac{u(\vec{r})}{k_bT} & \text{if } \vec{r} > 2r_0 \end{cases} \tag{48}$$

The integral of the potential can for this case be split up in two parts; the part for $r < 2r_0$ and the part $r > r_0$. Integrating a Taylor expansion of the potential then gives us the familiar Van der Waals equation:

$$P = \frac{Nk_bT}{V}\left[1+\frac{N}{V}\left(b-\frac{a}{k_bT}\right)\right] \tag{49}$$

where a and b are results of the integral; $a = 2\pi\int_{2r_0}^{\infty} d\vec{r}\vec{r}^2 u(\vec{r})$ and $b = \frac{2\pi}{3}8r_0^5$.
now the potential shows that it is assumed that the particles in this model are 'hard cored'. If the particles get too close, the potential diverges to infinity. They can never reach the exact same coordinates. This is in correspondence with the Pauli pressure, which has a very steep potential as well. As a reminder, we state here that the other two assumptions made were that only 2-particle interactions were relevant and that this only holds for low densities.

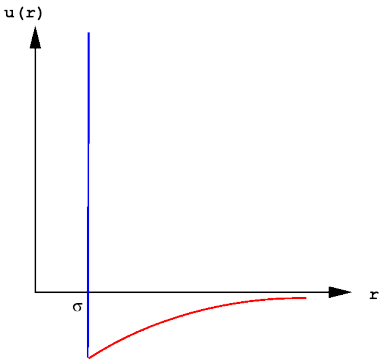

Figure 7: Van der Waals potential

This last assumption makes the Van der Waals EoS also invalid for neutron stars, as the densities are not sufficiently low. Because these equations however give a very insightful way in how particles interact due to different potentials, it still seemed useful to state the Van der Waals equation.

6.4 Polytropes

A polytrope is in general a thermodynamic process in the form of $pV^n = C$. For different values of n as a power in this equation, different types of processes can be modelled, such as isochoric or isobaric processes. A derivation for the equation of state of a polytrope will be given below, as for that we require the equations of stellar structure. From the polytropic equation, it is often easy to derive the relation between the central pressure or density and the total mass of the star involved.

Polytropes hence stem from solutions to the equations of stellar structure. They are not based on statistical physics, such as the previous interactions, but relate to phenomenological properties of the neutron stars. This is useful, since the behaviour of individual

particles in the neutron stars is not well understood. Also, the Van der Waals equation can only describe a small part of the entire system, as there are quite strict criteria for its assumptions to hold. It cannot deal for example with more than one phase of matter or superfluid neutrons just beneath the core of the neutron star for example. The polytropes are not affected by the still outstanding questions on the behaviour of these substances, as it is based on the equilibrium state of the stars and makes no assumptions on the subatomic interactions.

After looking at several ways to model interactions between particles, we have chosen to model the system using the polytropes. As will also be mentioned during a later chapter, a choice was made on modelling a star by adding baryon per baryon or modelling a star by adding lots of baryons at the same time. This difference implies a different look on the statistical physics; for the Van der Waals equation, one could very easily incorporate the first approach, while for the latter option (that we eventually went with), the polytropes are much more convenient.

7 The MIT-bag model

Because we are making assumptions on the behaviour of quarks inside the nucleus, it is useful to get a basic understanding of how quarks behave in a nucleon. In this thesis, it is assumed that they to not leave the boundaries of the nucleus, such that no QGP is generated. It is general knowledge that quarks are confined in a nuclei and that they are bound by the strong interaction, mediated by the gluons as force carriers. While quarks themselves have colour (say red, green or blue), the net colour of a subatomic particle must always be colourless or 'white'. Within a nucleon, the quarks obey Fermi-Dirac statistics. [2]

A simple way of modelling the behaviour of quarks within a nucleon is through the MIT-bag model. The MIT-bag model proposes that quarks are confined within a spherical volume and are exerting a pressure on a 'bag' confining this volume. The volume is not expanding because of the 'bag constant' B, that makes sure that a counteracting force is present. The MIT models actually stems from a model by Bogoliubov, at which we will first take a closer look.

7.1 The Model of Bogoliubov

Nikolay Bogoliubov made a proposal for modelling quark confinement in nucleons. He tried to realise this by giving the quarks a finite mass within the radius of the nucleon and an infinite mass outside of the nucleon [18]. Starting of from the Dirac equation for a massive particle within a spherical volume of radius R,

$$[\vec{\alpha} \cdot \vec{p} + \beta(m - V_s)]\,\psi = E\psi \tag{50}$$

and defining the eigenvalues for the angular momentum operators for $\vec{j^2}$, j_z and K cleverly using the operators $\vec{j} = \vec{l} + \vec{\sigma}/2$ and $K = \beta(\vec{\sigma} \cdot \vec{l} + 1)$ that commute with the Hamiltonian of the system, $H = \dot{\psi}\frac{dL}{d\dot{\psi}} - L$, we obtain the following wave function.

$$\psi_\kappa^\mu = \begin{pmatrix} g(r)\chi_\kappa^\mu \\ if(r)\chi_{-\kappa}^\mu \end{pmatrix} \tag{51}$$

Rewriting the Dirac equation to

$$\vec{\alpha} \cdot \vec{p} = E - \beta m + \beta V_s \tag{52}$$

and applying the momentum operator $\vec{p} = -i\hbar\nabla$ where we set $\hbar = 1$ and in spherical coordinates $\nabla = \hat{r}\frac{\partial}{\partial r} - i\frac{\hat{r}}{r} \times \vec{l}$ we find the following:

$$\vec{\alpha} \cdot \vec{p} = -i\vec{\alpha} \cdot \hat{r}\frac{\partial}{\partial r} + i\vec{\alpha} \cdot \hat{r}\,(\beta\,(K-1)) \tag{53}$$

Applying this operator to the wave function of Equation 51 and setting it equal to the right hand side of Equation 52, we find the coupled differential equations

$$(E + V_s - m)g(r) = -\left(\frac{\partial f}{\partial r} + \frac{f}{r}\right) + \kappa\frac{f}{r} \tag{54}$$

and

$$(E - V_s + m)f(r) = \frac{\partial g}{\partial r} + \frac{g}{r} + \kappa\frac{g}{r} \tag{55}$$

Now we need to define to potential V_s to keep the quarks in the region; we set

$$V_s = \begin{cases} m \text{ for } r < R \\ 0 \text{ for } r \geq R \end{cases} \tag{56}$$

Solving these equations, we find the solution

$$g(r) = \begin{cases} A\frac{\sin(Er)}{r} & r < R \\ A\frac{\sin(Er)}{r}e^{-\sqrt{m^2-E^2}(r-R)} & r \geq R \end{cases} \tag{57}$$

From this equation it can easily be seen that g decreases exponentially with the radius when the radius is larger than R. At the moment however, the quarks are still not confined. To achieve this, Bogoliubov let the mass parameter $m \to \infty$. Now the masses are confined to the region as the wavefunction dies of at $r = R$. This also shows the quantum constraints on the system, as the boundary conditions of this model are such that the wave function must be continous at $r = R$. One could continue to work on the energy of the ground state solution from these equations, but our purpose of showing where the quark confinement comes from has been accomplished and therefore we will not pursue that target.

A flaw of the Bogoliubov model was the fact that the radius of the spherical volume was built in manually instead of analytically determined. The lowest energy solution is namely the one where $R \to \infty$ This is one of the issues in the model that the MIT model tries to encompass in its approach.

7.2 A proposed solution to the infinite radius

The simplicity from the MIT bag model follows from its Lagrangian:

$$\mathcal{L} = \left[\frac{i}{2}(\bar{\psi}\gamma^\mu\partial_\mu\psi - (\partial_\mu\bar{\psi})\gamma^\mu\psi) - B\right]\theta_\nu(x) - \frac{1}{2}\bar{\psi}\psi\Delta_s \tag{58}$$

In this Lagrangian, B is an added universal constant called "The bag constant" and is an important parameter of the model. This parameter provides the additional energy density to keep the quarks confined in their volume. It can be shown that it is equal to a negative pressure working against the quarks, like the vacuum exerting a pressure on the volume of the nucleon. Δ_s describes the derivative of $\theta_\nu(x)$, which is a step function at the radius of the spherical volume. It is one inside and zero outside the bag. γ^μ represent the gamma matrices, which are a representation of the Clifford Algebra. They are defined by the anticommutation relation

$$\gamma^\mu, \gamma^\nu = \gamma^\mu\gamma^\nu + \gamma^\nu\gamma^\mu = 2\eta^{\mu\nu}I_{4\times4} \tag{59}$$

$I_{4\times4}$ being the four by four identity matrix. From an introductory course to RQM using [19], we know that we can apply the Euler-Lagrange equations to find the equations of motion:

$$\frac{\partial\mathcal{L}}{\partial\phi} - \partial_\mu\left(\frac{\partial\mathcal{L}}{\partial(\partial_\mu\phi)}\right) = 0 \tag{60}$$

First applying the left term of Equation 60 and putting in the respective field $\bar{\psi}$ instead of ϕ, we find

$$\frac{\partial\mathcal{L}}{\partial\bar{\psi}} = \left[\frac{i}{2}(\gamma^\mu\partial_\mu\psi)\right]\theta_\nu(x) - \frac{1}{2}\psi\Delta_s \tag{61}$$

The right hand side gives us

$$\partial_\mu\left(\frac{\partial\mathcal{L}}{\partial(\partial_\mu\psi)}\right) = \partial_\mu\left[-\frac{i}{2}\gamma^\mu\psi\theta_\nu(x)\right] = -\frac{i}{2}\gamma^\mu\partial_\mu\psi\theta_\nu(x) - \frac{i}{2}\gamma^\mu\psi n_\mu\psi\Delta_s \tag{62}$$

Filling these in for Equation 60, we obtain

$$\left[\frac{i}{2}(\gamma^\mu\partial_\mu\psi)\right]\theta_\nu(x) - \frac{1}{2}\psi\Delta_s - \left(\partial_\mu\left[-\frac{i}{2}\gamma^\mu\psi\theta_\nu(x)\right] = -\frac{i}{2}\gamma^\mu\partial_\mu\psi\theta_\nu(x) - \frac{i}{2}\gamma^\mu n_\mu\psi\Delta_s\right) \tag{63}$$

where n_μ is the vector normal to the sphere's surface. This long equation rearranges to

$$(i\gamma^\mu \partial_\mu \psi)\theta_\nu(x) + \frac{1}{2}(i\gamma^\mu n_\mu \psi - \psi)\Delta_s = 0 \tag{64}$$

Now we can start applying the boundary conditions and see what happens. First, we set Δ_s to zero and assume we are in the confined volume of the bag. The resulting equation is

$$i\gamma^\mu \partial_\mu \psi = 0 \tag{65}$$

We see that this is just the Dirac equation for a massless fermion!

$$(i\gamma^\mu \partial_\mu - m)\psi = 0 \text{ with } m \to 0 \tag{66}$$

At the point where θ_ν goes from one to zero, the derivative is infinite: $\Delta_s = \infty$. However, we know that

$$\frac{1}{2}(i\gamma^\mu n_\mu \psi - \psi)\Delta_s = 0 \tag{67}$$

Such that this must mean that

$$i\gamma^\mu n_\mu \psi - \psi = 0 \Rightarrow \psi = i\gamma^\mu n_\mu \psi \tag{68}$$

This also gives the complex conjugate,

$$\bar{\psi} = -i\gamma^\mu n_\mu \bar{\psi} \tag{69}$$

And now finally, to show that the quarks to not move outside of the volume, we show that the probability $\bar{\psi}\psi$ is zero:

$$-i\psi\gamma^\mu n_\mu \bar{\psi} = \psi\bar{\psi} = \bar{\psi}\psi = i\bar{\psi}\gamma^\mu n_\mu \psi \tag{70}$$

Since the terms are equal but of opposite sign, this must mean that they are zero! Depending on the bag constant, the energy densities at which the quarks deconfine is changing. As in this thesis the deconfinement and its accompanying phenomenology is not investigated, we will not discuss the model any further.

8 Equations of Stellar Structure

To determine the possibility of a star going to a quark star, we use the Tolman-Oppenheimer-Volkoff equations. These equations are the result of general-relativistic corrections to the simple Newtonian equations of stellar structure. The derivation of the general-relativistic version will not be discussed here, as it is outside of the scope of this paper. The Newtonian derivations however will be given below.
There are actually four equations of stellar structure: mass conservation (Equation 71), hydrostatic equilibrium (Equation 72), energy conservation (Equation 73) and energy transport (Equation 74).

$$\frac{dm}{dr} = 4\pi r^2 \rho(r) \tag{71}$$

$$\frac{dP}{dr} = -\rho(r)g(r) \tag{72}$$

$$\frac{dL}{dr} = 4\pi r^2 \epsilon(r) \tag{73}$$

$$\frac{dT}{dr} = \frac{1}{4\pi r^2 \lambda} L \tag{74}$$

Here, ϵ, λ and ρ are the energy output of the star for the shell with radius r and thickness dr, the conductivity proportionality constant and the density determined by the equation of state respectively [20].

The first equation, for mass conservation, is easily derived with help of Figure 8. The mass of the infinitesimal can be given as the sum of two components through

$$dm(dr, dt) = 4\pi r^2 \rho(r) dr - 4\pi r^2 \rho v dt \tag{75}$$

but since we are only interested in stable stars, we can leave out the time dependent part, divide by dr, and already obtain the desired equation:

$$\frac{dm(r)}{dr} = 4\pi r^2 \rho(r) \tag{76}$$

The derivation for the hydrostatic equilibrium is a little tougher, but can also be obtained through the help of the visual aid in Figure 9.

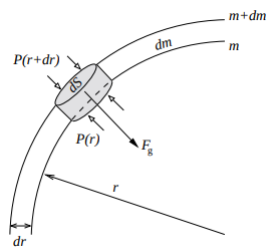

Figure 8: Visual aid for the derivation of the equation for conservation of mass. Taken from: [20]

In the visual aid, you see a volume element with surface area A and height dr and therefore volume V somewhere in the star. The curvature of the volume element in the star has not been taken into account due to the assumption that the curvature is negligible for such a small volume. The volume experiences several forces: the gravitational force pulling it downwards $F_g = g\rho V = g\rho A dr$. Also, there the pressure from below the volume compensating this gravitational pull, $P_{up}(r) = F_{up}(r)/A$. The pressure from above the volume element is slightly less, as the column of mass exerting a force on the volume is smaller by a length of dr. This gives an additional downwards pressure of $P_{down}(r+dr) = F_{down}(r+dr)/A$. Summing all these forces with the correct signs for their respective directions,

$$F_g + F_{down}(r+dr) = F_{up}(r) \Rightarrow g\rho A dr + P_{down}(r+dr)A = P_{up}(r)A \tag{77}$$

And by rewriting using $P(r+dr) = P(r) + \frac{dP}{dr}dr$:

$$g\rho(r)Adr + P(r)A + \frac{dP}{dr}drA = P(r)A \Rightarrow P(r)A = g\rho(r)Adr + P(r)A + dPA \tag{78}$$

$$\frac{dP}{dr} = -g\rho(r) \tag{79}$$

which is the equation that we were after.

For this derivation, the only equations of stellar structure that are used are Equation 71 and 72. It is difficult to use only one of these equations, as they are in fact coupled differential equations. Before we start to solve these equations however, we first need to consider whether the Newtonian regime is appropriate here.

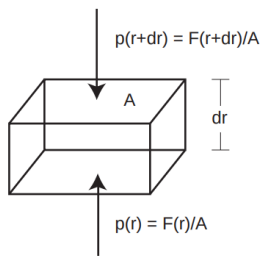

Figure 9: Visual aid for the derivation of the equation for hydrostatic equilibrium. Taken from: [20]

From the Fermi pressure for a relativistic electron gas, we know that the pressure is equal to

$$p_F(k_F) = \frac{\epsilon_0}{24}\left[(2x^3 - 3x)(1+x^2)^{1/2} + 3\text{arcsinh}(x)\right] \tag{80}$$

where $x = k_F/m_e c$. In the relativistic regime, we know that $k_F \gg m_e$ as for k_F [21]

$$k_F = \hbar\left(\frac{3\pi^2\rho}{m_n}\frac{Z}{A}\right)^{1/3} \tag{81}$$

The densities in the centres of neutron stars are on the order of $\rho_c = 10^{14}\text{g}\,\text{cm}^{-3}$ or $\rho_c = 10^{17}\text{kg}\,\text{m}^{-3}$. This means that in the centre of neutron stars, k_F is on the order of magnitude $10^{-19}\left(\frac{Z}{A}\right)^{1/3}$ where $m_e = 9 \times 10^{-31}$kg. Since the Fermi momentum is hence much larger than the electron mass, we need to consider relativistic effect for the densities involved in Neutron stars.

The relativistic equations for conservation of mass and hydrostatic equilibrium have been rewritten from the Einstein equations

$$G\mu\nu = \frac{8\pi G}{c^4}T^{\mu\nu} \tag{82}$$

using the Schwarzschild metric for a spherically symmetric mass. As mentioned before, the complete derivation for these relativistic equations will not be given, but can be found in e.g. [22] and [23]. They will just be given [24] below.

$$\frac{dm}{dr} = 4\pi r^2\rho(1+\epsilon/c^2) \tag{83}$$

$$\frac{dp}{dr} = -G(\rho(1+\epsilon/c^2) + p/c^2)\frac{m + 4\pi r^3 p/c^2}{r(r - 2Gm/c^2)} \tag{84}$$

We see that these equations are actually quite similar to the Newtonian equations - especially the mass, which has just a corrective multiplicative term. The pressure equation is a bit more complex, as several extra terms come in to play. We easily see that the additional terms only *contribute* to the original expression, such that the force of gravity is only strengthened by encorporating GR in the model. The two differential equations are also still coupled. Besides the equations being coupled, adding a level of difficulty to the integration process, we also still need an equation of state to determine the pressure-density relation. For this, we will use the polytropic equation of state.

8.1 Polytropes and Neutron Stars

To fully determine the mass-radius relationships of neutron stars, we need to assume an equation of state. Although more sophisticated models are available, the polytropic equation of state is a good approximation. The equation of state is as simple as

$$P = K\rho^{\gamma} = K\rho^{\frac{n+1}{n}} \tag{85}$$

where both K and γ are taken as constants for the model. For neutron stars or white dwarfs, values for n are often assumed to be $0.5 \leq n < 1$ such that $2 \leq \gamma < 3$ and K is on the order of 10^{-6} when doing the integration in cgs.

The polytropic equation of state has since its invention been superseded by more accurate models, but it is still popular due to its simplicity. It has also been shown to be still reasonably applicable for pressures over 10^{14}Pa or 10^{15}dyne cm^{-2} [25], such that we are in a safe region to use it in for the neutron star case.

The derivation for the polytrope is not very difficult, as it is just a combination of the first two stellar structure equations and some algebra. Starting by differentiating the hydrostatic equilibrium equation and putting in the mass continuity equation in the result, we find the following.

$$\frac{d}{dr}\left(\frac{1}{\rho}\frac{dP}{dr}\right) = \frac{2GM}{r^3} - \frac{G}{r^2}\frac{dm}{dr} = \frac{2}{\rho r}\frac{dP}{dr} - 4\pi\rho G \tag{86}$$

Collecting the pressure derivatives on the left hand side and dividing by r^2:

$$\frac{1}{r^2}\frac{d}{dr}\left(\frac{1}{\rho}\frac{dP}{dr}\right) + \frac{2}{\rho r}\frac{dP}{dr} = -4\rho\pi G \tag{87}$$

Now we fill in the equation of state: $P = K\rho_c^{1+\frac{1}{n}}\theta^{n+1}$ to obtain

$$\frac{1}{r^2}\frac{d}{dr}\left(r^2 K\rho_c^{\frac{1}{n}}(n+1)\frac{d\theta}{dr}\right) = -4\pi G\rho_c\theta^n \tag{88}$$

where now the not-so-obvious subsitution of $\alpha^2 = (n+1)K\rho_c^{\frac{1}{n}-1}/4\pi G$ is made to find

$$\frac{1}{\xi^2}\frac{d}{d\xi}\left(\xi^2\frac{d\theta}{d\xi}\right) + \theta^n = 0 \tag{89}$$

which is the familiar Lane-Emden equation [20]. This equation is only analytically integrable for specific values of the polytropic exponent $n \in \{0, 1, 5\}$, all specifying very specific models for the star, such as a star with an infinite radius or a star according to Eddington's assumptions [26]. Therefore, we have to integrate the solution numerically.

8.2 Integration process

The integration of the equations of stellar structure can be done in several ways. A simple option to use is just Euler's method, but this method is known to quickly diverge from the actual function and to be only accurate up to $\mathcal{O}(1)$, which means that the error in the integration process is proportional to the square in the step size. As we are interested in integrating over a large region and will not spend an enormous amount of time integrating in very little steps, this is not a suitable algorithm for our exercise.

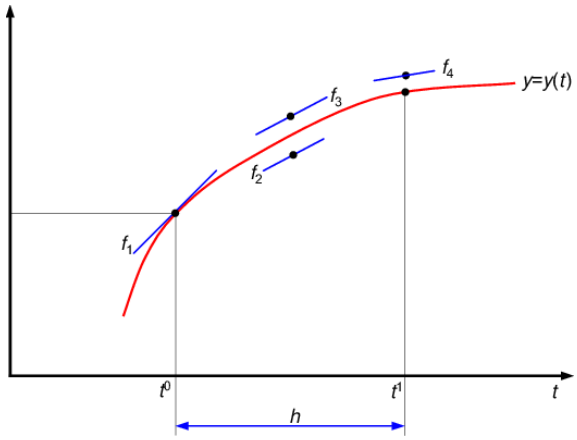

Figure 10: Visual aid for an overview of the Runge Kutta method. Taken from [28]

We make use of the Runge-Kutta 4th order Method. This method is described extensively in [27]. A short introduction however will be provided. A visual aid is given in Figure 10. Due to it being fourth order, it diverges much slower than Euler's method.

First, the slope of the function is evaluated of the point t_0. With this, an estimate is made where the function is at at $t_0 + h/2$, h being the difference between two points in the interval. This estimate is then evaluated again at $t_0 + h/2$, after which this estimate is used to make a final approximation about the end point of the function at $t_0 + h$. In its algorithmic form:

$$\begin{aligned} k_1 &= f(t_0, y_0) \\ k_2 &= f(t_0 + h/2, y_0 + k_1 h/2) \\ k_3 &= f(t_0 + h/2, y_0 + k_2 h/2) \\ k_4 &= f(t_0 + h, y_0 + k_3 h) \end{aligned} \tag{90}$$

And the final value for the approximation of y at $t + h$ is then given by the weighted average:

$$y(t + h) = y_0 + \left(\frac{1}{6}k_1 + \frac{1}{3}k_2 + \frac{1}{3}k_3 + \frac{1}{3}k_4\right) h \tag{91}$$

To solve the problem of the two ordinary differential equations being coupled, we iterate one step from the mass equation, determine the mass at this new step in the interval and then determine the next step for the pressure gradient. This is then used to determine the next mass gradient. Due to this procedure, there is an 'off by one' error, as the pressure of the previous radius is used to compute the mass of another, but this error is assumed to be insignificant.

The final thing that needs to be done is to determine the boundary conditions of the equation. This is a very simple process, if we know the central density or central pressure of the star (these can be determined from another by Equation 85. The central pressure is then given as $P(r = 0) = P_0$, where the pressure at the radius of the star is $P(r = R) = 0$. For the mass, we have similar boundary conditions: $M(r = 0) = 0$, while at $M(r = R) = M_*$. We can with these boundary conditions hence generate an array with radii symbolising the distance from $r = 0$km to the radius of the neutron star, who in general do not have radii over 20km. We stop integrating when the boundary condition is met, i.e. when the pressure is significantly small.

Integrating using the constants $K = 1.98183 \times 10^{-6}, \gamma = 2.75$ and different values for P_0, we get pressure- and mass profiles as given in the figures below. From all these figures, a final mass and a final radius can be determined. When we collect all these samples and

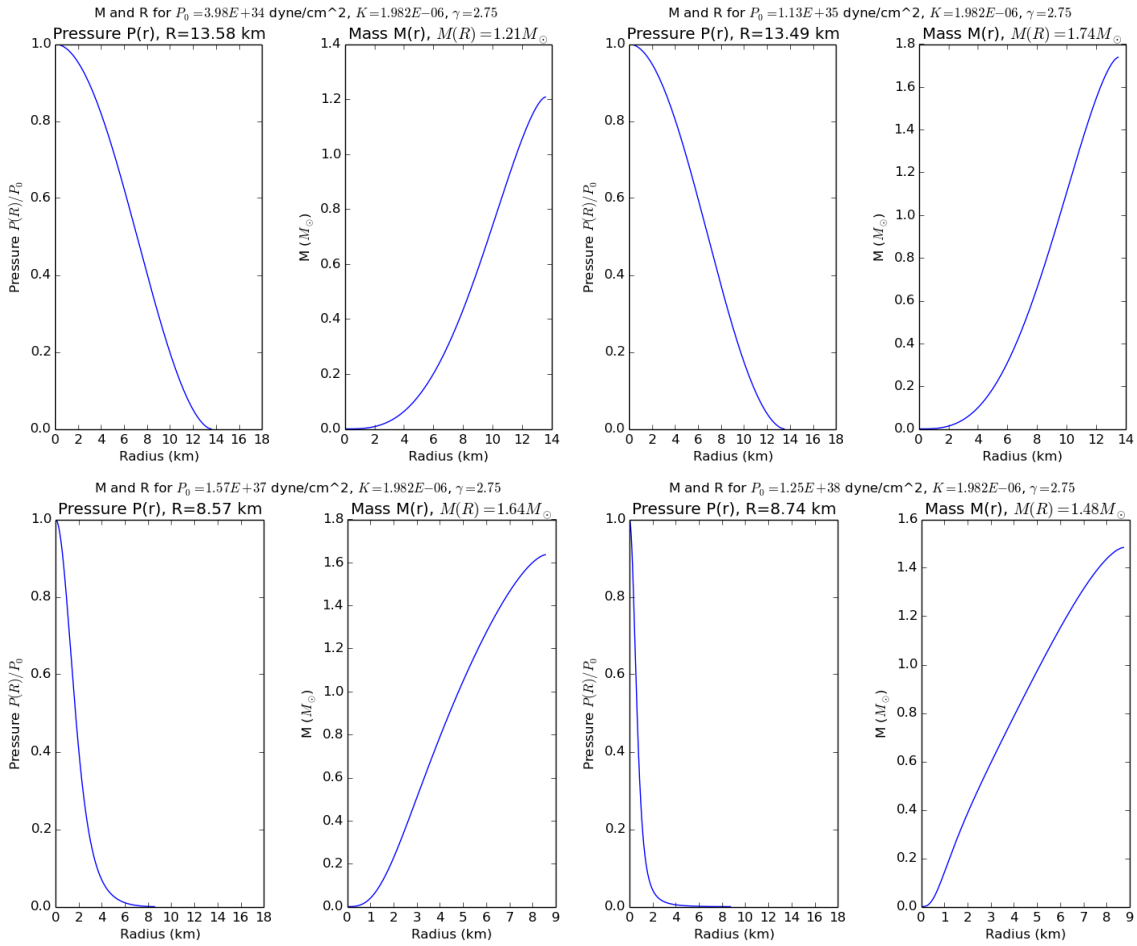

Figure 11: Pressure- and Mass profiles from neutron stars with a polytropic equation of state. The parameters for the eos are $K = 1.98183 \times 10^{-6}, \gamma = 2.75$, P_0 varying. More figures have been generated for other central densities, these can be viewed in the appendix.

plot them in a file, we obtain the M-R plot in Figure 13. This figure gives an overview of the possible configurations of stars with a certain mass - if these stars indeed follow the given equation of state,they need to be on the curve from the M-R plot. As can readily be observed, some configurations seem to be degenerate.

It is however important to know that we cannot blindly assume that all these results are physical. We have to take into account three important boundaries: the Schwarzschild radius [10], the causality boundary [29] and the Chandresekhar limit [11]. Once the stars get below their Schwarzschild radius,

$$R_s = \frac{2GM}{c^2} \tag{92}$$

they are collapsing to a black hole. This puts constraints on the average density of the star.

An even stricter boundary is the causality boundary. At the radius of the photon sphere - where the closest stable orbit for photons around a spherical object lies - causality starts to break down. Once a photon enters this region it can either remain on the radius of this photon sphere, which has a very small probability of happening, or spiral inwards to the black hole. The photon sphere radius is given by

$$R_{photon} = \frac{3GM}{c^2} = \frac{3}{2}R_s \tag{93}$$

These two event horizons are not the same. Massless objects can only travel at the speed of light and therefore have stable circular orbits around the mass. Massive objects, which can vary their speed, can have elliptical orbits that cross the photon sphere and have their orbit partly in the region between the photon sphere radius and the Schwarzschild radius. Figure 12 clarifies this explanation.

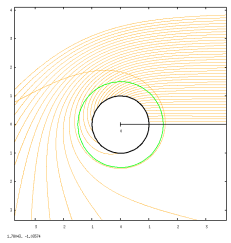

Figure 12: The green circle represents the photon sphere radius (only stable orbit), while the black circle is the Schwarzschild radius.

Also, for a neutron star to form, the supernova remnant needs to be at least heavier than $M = 1.44M_\odot$. When the star does not have a mass large enough, the degeneracy pressure from the electrons is large enough to maintain an equilibrium in the star, never actually making the chemical potential of the electrons large enough to start the electron capture process significantly. The star then ends up as a white dwarf.

Keeping these limits in mind, we still see a suitable configurations for these stars to form. Comparing these to literature [30] where several similar curves are drawn on the M-R plane (see Figure 14), we see that our results do not deviate greatly from the AP4 model and hence are credible.

8.3 Binding energies

What is an interesting next step, is to figure out what the binding energy per nucleon is in a star with these configurations. When the binding energy of the baryons is known, one can determine whether or not it is viable to convert normal matter to quark matter. To do this, we initially started off by just adding baryons to a spherical volume and checking what the binding energy of the system is. The binding of a particle added to a spherical mass was already given by Equation 4. A reasonable amount of particles to estimate for a neutron star would be 10^{57} particles. Generating these particles linearly on this scale would cause us to either have a very computationally intensive simulation, or

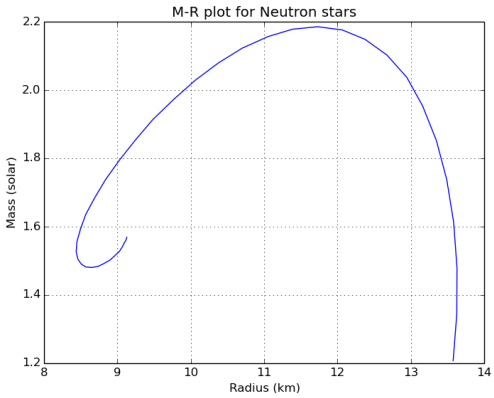

Figure 13: M-R plot from the pressure- and mass profiles from Figure 11

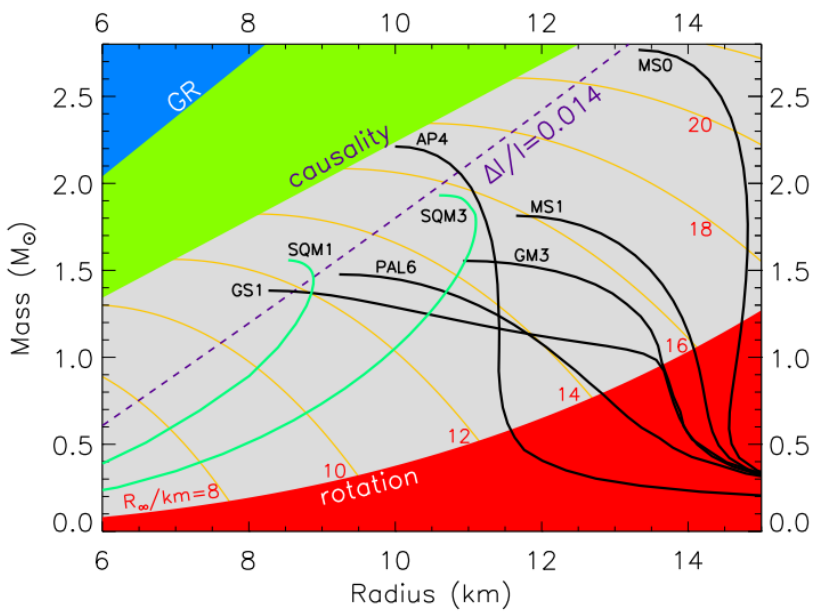

Figure 14: M-R plot obtained from [30]. Our curve in the M-R plane does not deviate greatly from the AP4 model.

otherwise loose some of the resolution of the simulation. A solution to this problem would be to generate the particles linearly in a logarithmic scale; this means that the particles are added in amounts of $10^{\Delta x/57}$, where Δx is the resolution of the simulation.

Setting the baryon mass to a constant and just adding the masses step by step while considering the added binding energy made us run into a not physics-related problem however - the dynamic range of Python variables. This model for determining the binding energy of baryons basically comprises adding more and more baryons in the most efficient way to a sphere (a packing factor of 0.74 [31]) and computing the binding energy on basis of the resulting geometry. This might work for a thought experiment, but is mathematically not feasible. This is because the mass does not increase quickly enough initially to fit within the simple model of only having gravitational binding. After several attempts to run the simulation with this hard sphere model, it was found out that the pressure was rising instead of declining for increasing radii. This is of course not what was expected, and the problem appeared to lay in the effective mass of the additional baryons. Briefly looking forward to Equation 95 (a derivation will be given there), we found that the derivative $\frac{dM}{dB}$ got negative, meaning that you were removing mass from the neutron star by adding more baryons. This is of course not a physical solution, but the numerics indeed showed that $\frac{GM}{r} \leq 1$ during the iterations. At around 10^{24} baryons the script started throwing dynamic range overflow errors, not even close to the desired number of baryons. Hence, we had to look for a different solution. The fact that this problem occurs, might also be a hint that the optimal spherical volume packing is not efficient enough to form these kinds of compact stars, and supernuclear densities are required.

To overcome this issue, we took a completely different approach than what was just proposed. Using the generated pressure-radius relations in solving the TOV-equations, we could determine the binding energies per shell of the neutron stars. This has several advantages: not only does it solve the problem from the previous paragraph, it also resembles a more complicated system as the EOS that was used to generate this data does take the strong force into account!

Importing the results of the solution for a particular neutron star configuration, one can determine the density of the shell using the equation of state (Equation 85) and determine the baryonic mass of the system. As the equations of stellar structure have no explicit dependence on the mass of the particles - it is purely phenomenological - we can use the solutions for different compositions. The mass that is computed by integrating the Equation 71 is just the gravitational mass - the binding energy is not considered, as this has no influence on the equilibrium structure of the star.

The number of particles in the specific shell is then assumed to be the mass of the shell divided by the baryonic mass of the particle. The binding energy of the system with the added shell is then considered to be the binding energy of the previous shell, minus (as the binding energy is negative) the number of particles times the added binding energy per particle from Equation 4. This is derived from the following steps. The mass for a star with one baryon more than the original is given by

$$M(B+1) = M(B) + m_B - \frac{GMm_B}{Rc^2} \tag{94}$$

$$\frac{dM}{dB} = m_B - \frac{GMm_B}{r} = m_B\left(1 - \frac{GM}{r}\right) \tag{95}$$

$$\frac{dM/m_B}{dB} = 1 - \frac{GM}{r} \tag{96}$$

The total mass of the star would then be given by

$$m(r) = \int_0^r 4\pi r'2\rho(r')dr = Nm_B - \int_0^m \frac{Gm'm_B}{r}dm' = N\left(m_B\left(1 - \frac{Gm}{r}\right)\right) \tag{97}$$

From this equation, we can derive the number of baryons up to a shell:

$$N(r) = \frac{m(r)}{m_B\left(1 - \frac{Gm(r)}{r}\right)} \tag{98}$$

The results from this approach entail more than just the binding energy of the system; the binding energy per baryon can also easily be determined, as the number of baryons in the system is dynamically determined from the density of the shells. An example result of such a computation for one specific configuration is given in Figure 15. It has to be said that during this process, the strong interaction between the particles in the shell is neglected. Quantitatively, this means that the binding energy would most likely be even lower than it is now. In making the step from the mass density to the baryon number, we did assume

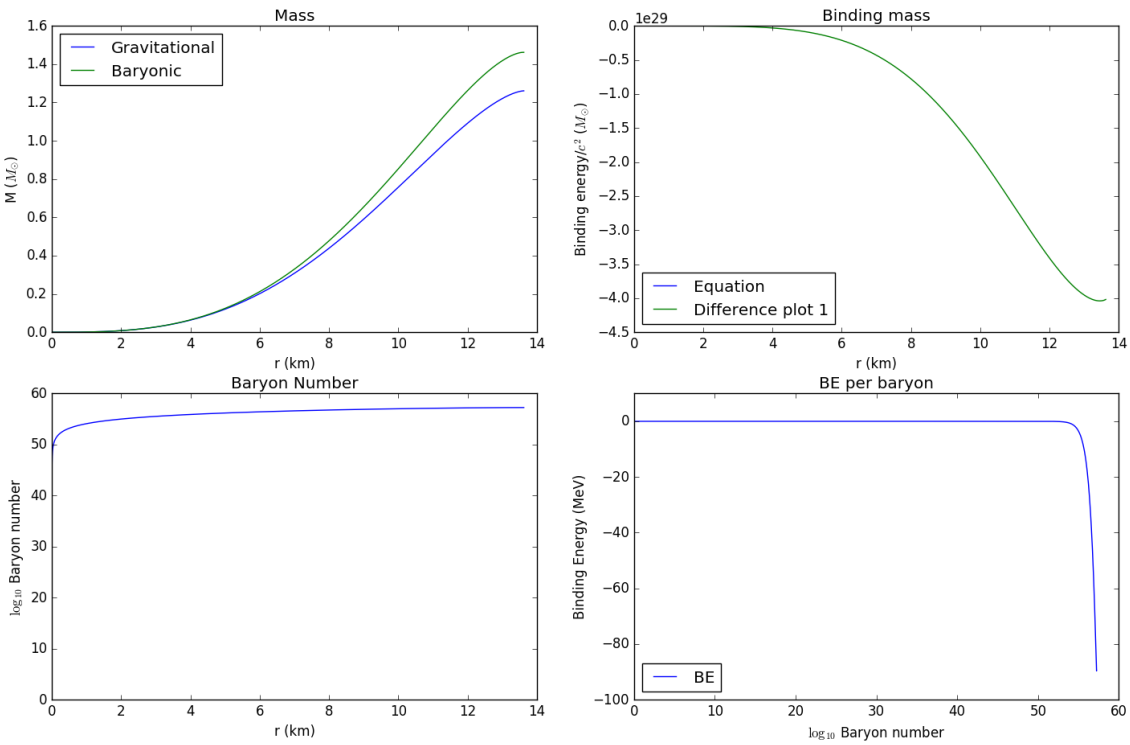

Figure 15: The mass of a star enclosed within a radius r, the binding mass within a radius r, the number of baryons within a radius r and the binding energy in MeV per added baryon.

the mass of the baryon. To determine whether there are any smooth transitions from the neutron star to a compact star with different baryonic constituents, we simply replace the baryon mass by that of a heavier particle. The masses that were used for the particles are given in Table 1.

Actually, both the lambda and sigma baryon are part of a broader set of baryons. The difference between the two sets lies in the behaviour of the wave function under the exchange of the third quark in the baryon; both lambda and sigma baryons exist of a combination of up- and down quarks and one quark of a heavier doublet. The sigma baryon is asymmetric under flavour exchange of the third quark, while the lambda baryon

Particle	Composition	Symbol	Mass (MeV c^{-2})	Mass (kg, $\times 10^{-27}$)
Proton	uud	p	938.272046	1.6726
Neutron	udd	n	939.565379	1.6749
Lambda	uds	Λ^0	1115.683	1.9889
Sigma	uus	Σ^+	1189.37	2.1202

Table 1: Brief summary of the baryons used in the analysis. Data taken from the Particle Data Group [32].

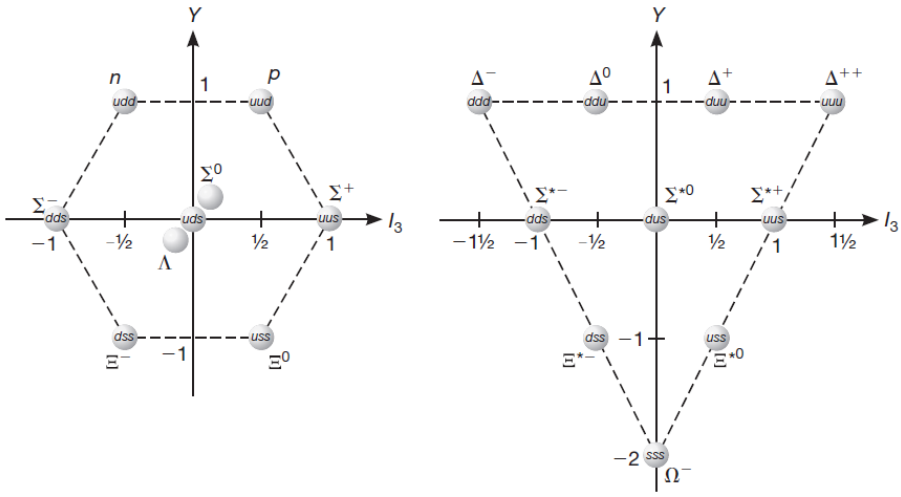

Figure 16: The baryon octet and the baryon decuplet. Taken from: [2].

is symmetric. Even though they may sometimes be constituted of the same quarks, such as the charmed sigma Σ_c^+ (udc) and Λ_c^+ (udc).

An explanation for this can be found in the representation theory of the wavefunction for the baryons. A basic understanding of group theory is required to make the following argument. If the reader is unfamiliar with irreps, one could read *Groups, Representations and Physics, Chapter 3 and 4* [33]. This situation is similar as for electrons having spin - the irrep of the product of the two electrons gives a singlet spin state and a triplet spin state.

$$\begin{pmatrix}\uparrow\\ \downarrow\end{pmatrix} \otimes \begin{pmatrix}\uparrow\\ \downarrow\end{pmatrix} = \begin{pmatrix}\uparrow\uparrow\\ \uparrow\downarrow + \downarrow\uparrow\\ \downarrow\downarrow\end{pmatrix} \oplus (\uparrow\downarrow - \downarrow\uparrow) \tag{99}$$

We can do something similar for the representation of the first two quark families (while leaving out the charmed quark):

$$\begin{pmatrix}u & \\ d & s\end{pmatrix} \otimes \begin{pmatrix}u & \\ d & s\end{pmatrix} = \begin{pmatrix}uu & & \\ \frac{ud+du}{\sqrt{2}} & \frac{us+su}{\sqrt{2}} & \\ dd & \frac{ds+sd}{\sqrt{2}} & ss\end{pmatrix} \oplus \begin{pmatrix}\frac{ud-du}{\sqrt{2}} & \frac{us-su}{\sqrt{2}} \\ \frac{ds-sd}{\sqrt{2}} & \end{pmatrix} \tag{100}$$

Now there's also still the multiplication of this irrep with the third quark and with the spin representations (as the quarks are fermions themselves as well). Working this out completely would finally give us a combination of a quark decuplet and a quark octet, the decuplet having a spin of 3/2 [34] and the octet having spin 1/2, see also Figure 16. Having higher spin creates more possible states, but also means that the system is in a higher energy, therefore containing heavier particles.

Putting in the masses from Table 1 into the simulation and plotting the binding energies per nucleon into an overview, we find the following figure. In these figures, we see that

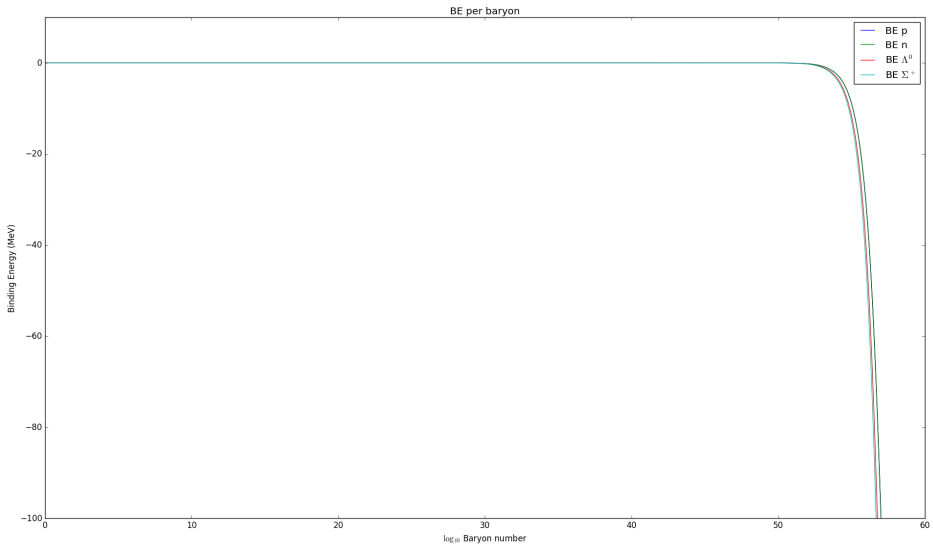

Figure 17: Binding energies per added baryon for the first up to $\approx 10^{57}$ baryons.

the binding energy for heavier baryons keeps decreasing (i.e. getting more negative). Just as for nuclei, this means that if there is a decay path from the lighter nuclei to the heavier nuclei, it could be energetically favourable to convert the neutrons to Λ^0or Σ^+ particles. In Figure 19, we also see that the number of required baryons to make up for the mass of the star is smaller for heavier baryons. The baryon number differs a factor of $10^{57.1121}/10^{57.0327} \approx 1.1882$ for the neutron and the baryon, while the mass ratio of the two is also $m_{\Lambda^0}/m_n \approx 1.1887$ - a difference of only 0.0005. The fact that these ratios are so comparable is probably due to the fact that we're assuming the same solution for the new quark model. This while the interaction between the neutrons and the lambda baryons is completely different. They possess different quantum numbers; for the neutron, the strangeness is zero, while for the lambda baryon it's -1. The isospin for a neutron is -1/2, while for a lambda baryon $I_3 = 0$. This means that the strong interaction should be modelled differently than for just similar neutrons. Using the polytropic solutions of the TOV-equations, this fact is ignored and the only difference is in the mass of the particles.

A proposed solution is making a new, quantitative modification to the pressure-density relation. From [35], concentrations of up to $\frac{n_\Lambda}{N} = 0.4$ have been found. If these Λ^0 can now physically overlap the neutrons due to the different quantum numbers, we can argue that we can model the system as two weakly interacting gasses. This does however mean that the density in the star goes up; the volume shrinks, as there are now more baryons per volume. To keep the model simple, we assume that the baryons follow the same $\rho(r)$, but just with a different normalisation. We can then just scale the density at every point as $\rho(r) = \frac{N}{n_{\Lambda^0}}\rho'(r)$.

For the concentrations $\frac{n_{\Lambda^0}}{N} \in \{0, 0.1, 0.2, 0.3, 0.4\}$, the M-R plots are recalculated. These curves are then combined into one figure, resulting in Figure 20. In Figure 20 we see that there are multiple points in which these configurations intersect.The fact that at this resolution the curves are already shown to intersect suggests that there is a continuous transition from no lambda baryons to a significant concentration.

No plot has been made for larger concentrations of strange baryons, on the arguments that the processes that convert the neutrons to lambda baryons are limited by the chemical potential of the constituents and the increasing energy that is required to overcome the Fermi barrier. Also, other baryons such as the sigma baryons are starting to appear and

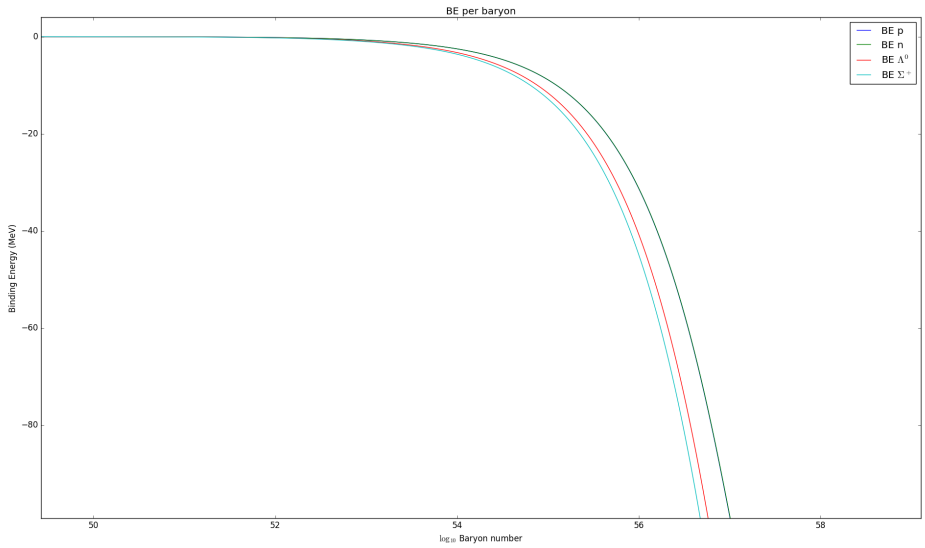

Figure 18: A close up of the more interesting part of Figure 17

the simplified two-phase model starts to give up.

The current model of the star contains several flaws. Proposals for fixing these flaws were done, but rejected. The first consideration was to model two stars separately and 'stick' them onto each other. If you want to model a 2 $M_\odot$ star for example, one knows what the central densities are for two separate stars that make up the mass if one 2 $M_\odot$ star through the previous simulations. If these are then stuck onto each other, the densities can be determined to find the model of the star where the radius of the lambda baryons is confined to a smaller radius. The flaw in this train of thoughts is that a compact star with this equation of state and such a low central density might not even represent a realistic physical system. A pressure resulting in a 0.6 $M_\odot$ star has never been found in actual neutron stars, even though over 2000 stars are known.

The flaw in the chosen solution is that although we know that the lambda baryon density is not as widespread throughout the star as the neutron density, we have chosen to just apply a multiplicative factor in the density profile. A better solution would be to model the lambda baryon density up to a certain radius, after which the density profile is completely taken over by neutrons.

The third proposed solution was to model the density as a function of the radius based on the concentrations of the different baryons. In the centre of the star, the largest concentration of lambda baryons is expected. Here, the concentration consists hence approximately of 40% Λ^0 and 60% neutrons. The Λ^0 concentration decays outwards, and we could have chosen the Fermi function to model the concentration gradient from the centre outwards:

$$F(\epsilon) = \frac{1}{e^{((\epsilon-\mu)/kT)} + 1} \tag{101}$$

From this, we only have to determine a reasonable point where we expect the chemical potential μ to be equal to the energy of the baryons, ϵ. We could say that this is at $0.75R_*$, based on Figure 23.

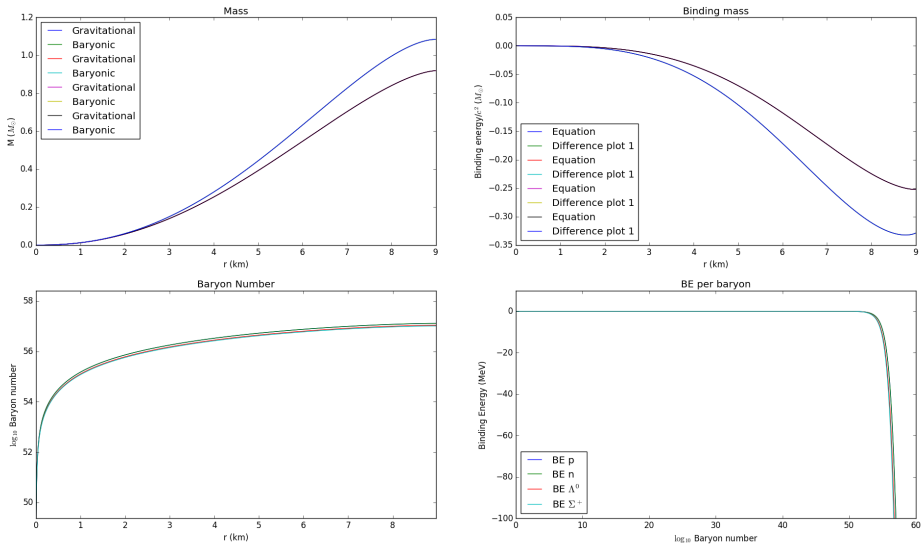

Figure 19: Mass-radius relation, binding mass within radius, baryon number and binding energy per baryon for four different baryons.

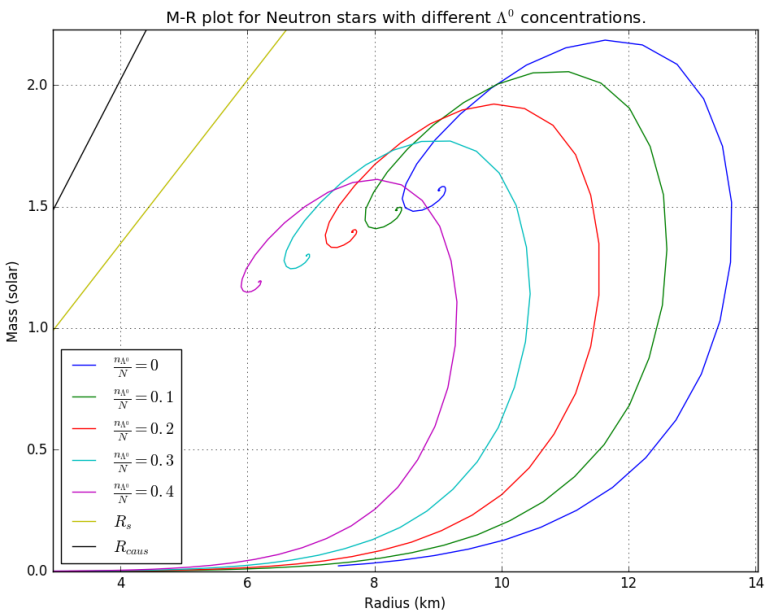

Figure 20: M-R curves for different concentrations of Lambda particles. In the left top, the causality condition and Schwarzschild radius are shown. As can be seen in the figure, all configurations are still slightly below these margins.

9 Observational properties of Quark Stars

So far we have been theorising the existence of strange stars. To confirm whether or not these stars also exist in the universe, one could try to perform statistics using star surveys; observations of basic characteristics of a lot of stars such as their mass, radius, and emission spectra. But how would one differentiate a strange star from a regular neutron star of pulsar? This question is answered using some observational methods for determining the mass and radius of neutron stars, such that we can check where the observed stars are in the M-R plot and whether they are in the normal neutron star region, or the region inhabited by strange stars.

9.1 On the Angular Momentum of Quark Stars

Another way to detect the presence of a quark star is to look at the Angular Momentum. The difference between quark stars and neutron stars lies in the difference of the moment of inertia. First, let's show the principle in computing the moment of inertia for a solid, constant density sphere. Remember that the moment of inertia is

$$I = \int r^2 dm. = \int r^2 \rho(r, \theta, \phi) dV \tag{102}$$

For a infinitesimally thin disk with constant density, we get the moment of inertia

$$I = \int r^2 dm = \int_0^R r^2 \rho dv = \int_0^R r^2 \rho (2\pi r) dr = 2\pi\rho \int_0^R r^3 dr = \frac{2}{4}\rho\pi R^4 = \frac{M_{disk} R^2}{2} \tag{103}$$

Now for the moment of inertia for a solid sphere with constant density, we stack disks onto another over the same axis, with a radius ranging from $R = 0$ to $R = R_{sphere}$.

$$\begin{aligned}
I_{sphere} &= \int \frac{1}{2} M_{disk}(z) r(z)^2 \\
&= \frac{1}{2}\pi\rho \int_{-R}^{R} (r(z))^4 \\
&= \frac{1}{2}\pi\rho \int_{-R}^{R} (R^2 - z^2)^2 \\
&= \frac{1}{2}\pi\rho \int_{-R}^{R} \left(R^4 - z^2 R^2 + z^4\right) dz \\
&= \frac{\pi\rho}{2} \left[R^4 - R^2 z^2 + z^4 \Big|_{-R}^{+R} \right] \\
&= \frac{\pi\rho}{2} \left(\frac{16 R^5}{15} \right) \\
&= \pi\rho \left(\frac{8 R^5}{15} \right) \\
&= \frac{2}{5} M_{sphere} R^2
\end{aligned} \tag{104}$$

where we have used that $M_{sphere} = \frac{4\pi R^3}{3}$ and that the radius of the disk is given through $y^2 = R^2 - z^2$.

We know that the angular momentum relates to the moment of inertial through the equation $L = I\omega$. If we have a process that converts energy into mass, such as the transition from normal matter to exotic matter in the form of strange quarks, we therefore have a decreasing rotational velocity ω as the angular momentum L is a preserved quantity.

Therefore, if we know what the transition rate of mass to energy is, we are able to determine that change in angular velocity of the star. We suppose therefore that a neutron star in the phase of converting normal matter to quark matter is slowing down.

For a sphere with a varying density throughout the sphere as a function of radius, that is, $\rho = \rho(r)$, things get a little more complicated.

9.2 Volume occupation

In this section, we will give a quantitative argument about the volume change of the neutron star as it converts to quark star. We know that by Pauli's exclusion principle, we cannot have two fermion occupy the same volume. If we assume that the star consists of two types of fermions completely, we know that we can decrease the volume of the star by adding another fermion. If we go to an equilibrium of just up and down quarks to up, down and strange quarks, we can contain the same mass in a volume $\frac{2}{3}$ of the original volume. If we again look into the moment of inertial, we see that the moment of inertia decreases by a factor of $\frac{4}{9}$, meaning that the rotational velocity is going up by a factor of $\frac{9}{4}$. Although determining the exact radius of a neutron star is hard, they can be determined from binary systems. Since mass-radius relations are relatively confined for neutron stars, a decrease in volume by 2/3 can be noticed. When such a discrepancy is found between a known curve in the M-R relations, it might be a hint towards strange stars.

9.3 Average density of pulsars

Through the rotational velocity of a pulsar, we can actually set an estimate to the average density of the star. We know that the rotational kinetic energy can never be higher than the gravitational potential of the star - otherwise, the star would shed off matter. We know that the gravitational potential of the star is equal to $U = \frac{GMm}{R}$ where M is the mass of the star, m is the mass of the 'test object' and R is the radius of the star. Furthermore, the rotational kinetic energy is equal to $\frac{1}{2}m(\omega r)^2$. Equating these and performing algebra, we see

$$\frac{m(\omega R)^2}{2} = \frac{-GMm}{R} \Rightarrow \frac{4\pi^2 R^2}{2P^2} = \frac{-G4\pi R^3 \bar{\rho}}{3R} \Rightarrow \bar{\rho} = \frac{3\pi}{2GP^2} \tag{105}$$

where P is the period of the pulsar. From observations of pulsars we can then determine the average density of the pulsar. For example, if we look at the crab nebula, with a rotation period of 33ms, we find an average density of $\bar{\rho} = 6.484 * 10^{10} \mathrm{g\,cm^{-3}}$.

9.4 Quark Nova

A proposed phenomenon when a neutron star is converted to a quark star is the quark nova. When the quarks might deconfine during the spin down of the neutron, a lot of energy is released - as much as $10^{47} J$. The remaining quark star is of a mass on the order from $0.3 - 1 M_{\odot}$. The energy released in the process might be the cause for some of the gamma ray bursts observed in the universe. At around a nuclear density of $7\rho_N$, with a bag energy of $B_{conv} = 50$MeV per baryon, its contents are more than 5.5 times as strongly bound as those of the Fe-56 nucleus, and therefore very stable [36].

9.5 Gravitational redshift

From general relativity, it is known that time passes slower when you are near large masses. For photons, this means that when they move away from a large mass, such as a compact star, they experience time going faster over the course of their lifetime. The result of this

is that the photons will decrease in frequency; they will become 'redder'. The redshift due to this effect can be given through

$$lim_{r\to\infty} z(r) = \frac{1}{\sqrt{1-\frac{r_s}{R_e}}} - 1 \tag{106}$$

where r_s is the Schwarzschild radius of the object and R_e is the radius of emission of the photon. When the masses of the neutron stars are hence determined by other means, such as the Shapiro delay, one can now constrain the radius of the neutron stars as most of the photons that are emitted come from the neutron star outer crust. With this radius determination, the volume change described in the previous section can for example be observed.

9.6 Gravitational wave observations

Since the first observations of gravitational waves were made by the LIGO collaboration, propositions have been made to look for traces of neutron stars in the gravitational waves as well. The first famous gravitational wave observation, GW150914, was attributed to two merging black holes. Gravitational waves can also be produced by the merging of two neutron stars, as these masses also have a large influence on the behaviour of spacetime.

The first probable neutron star-neutron star merger was observed in event GW170817 in NGC4993 [37]. The masses of the binary object were not very likely to be of black holes. What further manifested the confidence in a binary neutron star merger was the observation of a gamma ray burst only 1.7s later by Fermi GBM, at the same location. These highly energetic radiation bursts were theoretically already associated with neutron mergers.

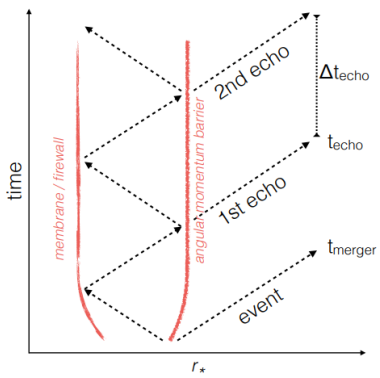

Figure 21: In this graphic, gravitational waves are reflected by the proposed 'membrane' or 'firewall' of a black hole, that is supposed to solve the famous information paradox. For a neutron star, this will just be the neutron star itself deflecting the gravitational wave.

The fact that we can say with reasonable confidence that this event is attributed to two neutron stars is not the main point of this paragraph. It is proposed from derivations from general relativity that heavy spherical bodies, such as neutron stars or black holes, possess an event horizon known as the photon sphere. These have already been discussed previously while putting constraints on the masses of the neutron stars, see Equation 93. The photon sphere is an effect of the curvature of spacetime by the mass, influencing the null-geodesic or often called 'light-like' trajectory of light on spacetime. Gravitational waves follow these same geodesics, as they are not massive particles moving through time, but ripples of spacetime itself. The effect of massive objects on gravitational waves is therefore the same as on light.

When Eddington performed the first observation of gravitational lensing during an eclipse, he computed the deflection of photons by the equation

$$\alpha = \frac{4GM}{c^2 d} \tag{107}$$

where α is the deflection angle in degrees and d the impact parameter. To obtain a mirror-like effect for gravitational waves, i.e. $\alpha \approx 180°$, one wants a small impact parameter and a large mass. This is exactly the kind of environment that these compact stars represent. Proposed is therefore a mirror-like effect that influences how we observe the gravitational waves [38].

Gravitational waves emitted during the neutron star merger are partly reflected by the photon sphere of the neutron star and head back to the neutron star. Neutron stars, as opposed to black holes, cannot absorb significant amounts of energy from these waves like black holes can. Instead, the waves are partially reflected back to the photon sphere, after which this process iterates. A representation of this process is given in Figure 21. The echoes of this process can be observed and using the time interval between the signals, the mass of the neutron star can be constrained.

9.7 Shapiro delay

Currently, Shapiro delay is one of the most accurate ways to determine the mass of a neutron star. It is based again on general relativity, where the time that light (or electromagnetic radiation) takes to get from a source to its observer is determined by the geodesic through spacetime. When a neutron star has a companion where the shared orbital plane is nearly edge-on the earth, it is possible to observe this effect. When the companion is near the line of sight to the star, the geodesic gets longer due to the influence of the companions mass on spacetime. This effect can be observed in the peak luminosity timings of neutron stars.

The effect was proposed by Irwin Shapiro in 1964 [39] and is based on the Schwarzschild metric for spherically symmetric massive objects. He originally tested his hypothesis by bouncing radio signals past the sun to Venus and catching the signal, while measuring the delay with respect to flat space. The delay that he found, approximately 2×10^{-4}s, was confirming his computations [39].

This effect has been used on determining binary systems of neutron stars. One of the most heavy neutron stars found so far, PSR J1614-2230, was analysed in this way. In figure 22 the received radiation delay from the pulsar is shown. The period of the companion around the neutron star is around 8.7 days, which is normalised on the x-axis of the figure. The yellow beam represents the radiation pointing towards earth, the red circle is the pulsar and the blue circle is the white dwarf.

At orbital phase 0.25, a sudden peak occurs in the pulsar signal. The top panel shows no corrections - this is just the raw signal. The middle panel shows the best fit model for a non-relativistic theory, where this model was found using χ^2 minimisation. The bottom panel shows optimisation including GR-effects. One can see that the signal from the middle panel looks a lot less like the Gaussian noise that is expected when this effect does not occur and an acceptable noise level when the shapiro effect has been taken into account in the third panel.

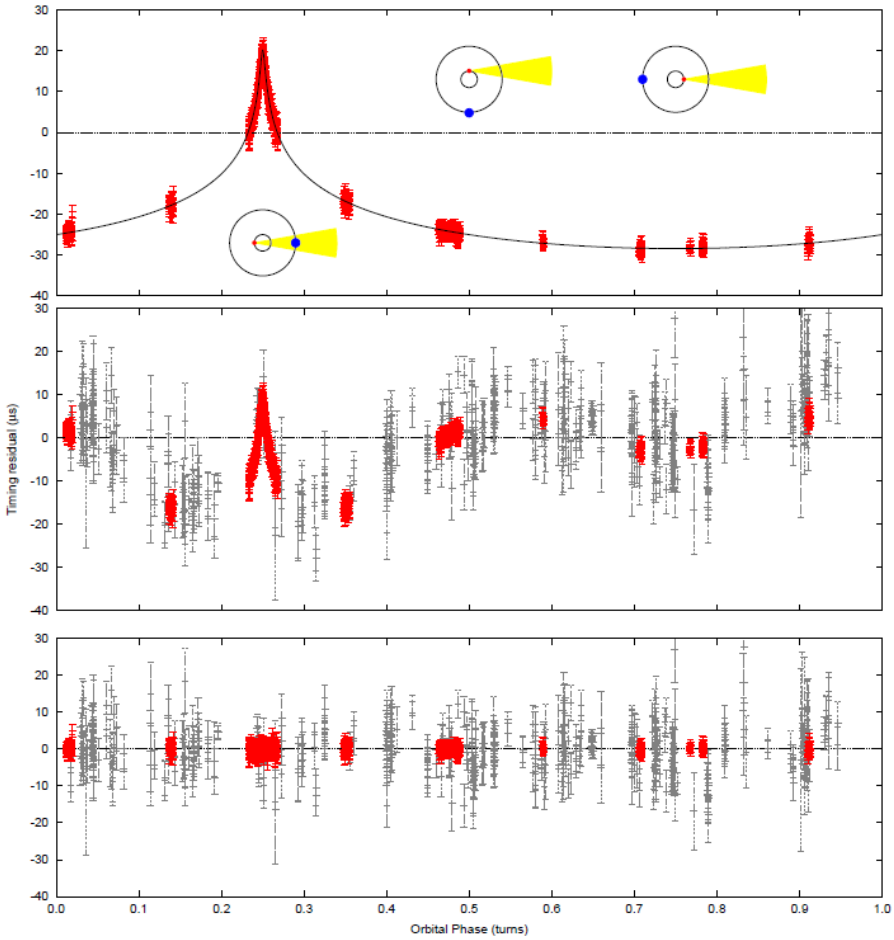

Figure 22: Visual representation of one delay cycle. Taken from: [39]

10 Conclusion

In this thesis, we have looked at the possibility of the existence of stable quark- or hybrid stars. To do so, we have solved the Tolman-Oppenheimer-Volkoff equations for a polytropic equation of state and varied its initial conditions such that mass-radius relations for a lot of different neutron star configurations were obtained.

Using these relations, the density-radius relations was determined. Using the densities of the 'infinitesimal' shells, we were able to determine the binding energy of the quark star in general and the binding energy per baryon.

In Section 3.2, an estimate was made for the binding energy of a neutron star as if it adhered to the liquid drop model or semi-empirical mass formula. A binding energy of $BE \approx 10^{57}$MeV was found for this quick estimate. The binding energy that was determined by solving the equations gave a 'binding mass' of about $0.4\mathrm{M}_{\odot}$, which corresponds to $BE \approx 10^{59}$MeV. For a ballpark estimate while completely ignoring the purpose of the liquid drop model, it seems that these results are credibly close.

Using the current model, it seems possible that strange stars exist. As there clearly exist overlap regions where all assumptions for the underlying equations holds, it looks like there is a degeneracy for a regular neutron star and a strange star. If the processes involved in these transitions are indeed not limited, this could lead to high concentrations of hyperons inside the star. Due to these conversions to hyperons, the volume of the star is allowed to shrink by an expansion of the available number of quantum numbers.

One could now try to argue that from this argument it is clear why neutron stars convert to black holes, but that is a bit too soon. One should try to find out what the equilibria for the baryons are and how this affects the structure of the star. The model used for this project was so crude that this conclusion would not be justified.

Additional notes that have to be made are that just one type of hyperon, the Λ^0 baryon, was considered in this model and that we only tested the model for one set of polytropic parameters K and γ. It was found for example that the concentrations of baryons converge to some percentage of the population for up to 1.2 times the nuclear mass.

The alternative model, where the presence of the baryons is varied throughout the models both in concentration as a function of radius and ratio of hyperons to baryons, would have been more appropriate. Using the Fermi equation, we would probably have been able to give a better estimate of the actual masses and radii of these strange stars.

The intersections in the current M-R plot lie on a curve where hyperons can be formed in the dense regions of the neutron star. If the trajectory of the configurations is followed towards the end of the curve (from right to left), the concentration of Λ^0 baryons will increase. However, with just neutrons and lambda baryons, the volume of the star will not shrink enough such that it becomes a black hole yet. This method does however unreasonably assume that the density distributions of the strange baryons and the neutrons are the same throughout the neutron star up to a multiplicative factor.

11 Outlook

In the main part of this thesis, it has been assumed that there is only one type of baryon present in the star. Whether it was neutrons, Lambda -, or Sigma Particles, this is of course not a realistic version. One can argue however, that the actual solution is somewhere in the middle. As can be seen in Figure 18, the binding energy per added baryon for Lambda particles for this EoS is lower than that of neutrons. In a realistic scenario, the real binding energy is probably in between these two extremes.

An argument can be made on the equilibrium concentrations of the particles based on known properties of the baryons. The fact that the isospin of the Λ^0 particle is zero for example, makes that it is probably more prominent in the mixture than the Σ^+ particle, which has an isospin of 1. Their contributions can however not be ignored, such that the equilibrium condition is, again, somewhere in the middle of these extremes.

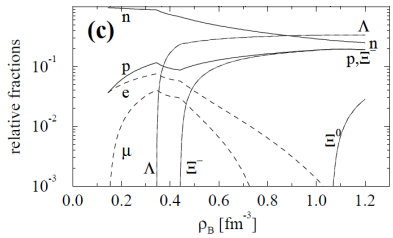

Figure 23: Hyperon concentrations in Neutron stars for similar central pressures. *Taken from: [35].*

A nice next step in the process of finding whether a hybrid star is an actual possibility is considering different pressure-density relations, that also take into account multiple phases at the same time. In other research, it has been shown that the presence of multiple hyperons at the same radii is not insignificant, see for example Figure 23 [35].

In this thesis, only the contributions of neutrons and Λ^0 have been considered, where the protons still have a significant contribution as well. If the protons would not be present, the chemical potential would be too low for the neutron star to be stable, and it would start to decay through the beta decay process. Also, the contributions due to e^-, μ, Ξ and possible pion and kaon condensates can be encorporated in a more sophisticated model.

Acknowledgements

I would like to thank both my supervisors, prof. C. J. G. Onderwater and prof. dr. R. M. Mendez for their effort in this project. Whether the issues at hand were on connecting Physics and Astronomy as separate topic into one thesis, administrative, or of physical nature, they were always willing to help me out.

Furthermore, I would like to thank R. van de Weygaert for his patience as a Thesis coordinator, as I realise that my planning and administration was not the most convenient for the organisation of all bachelor theses.

Finally, I would like to show my gratitude regarding the tolerance of my fellow board members at the FMF. Although I sometimes was quite irritable and stressed around them while fulfilling my responsibilities there, they almost never mentioned their displeasure with how I prioritised my tasks. The fact that they kept me filled up with coffee was also very helpful.

References

[1] W. Baade and F. Zwicky, "Remarks on super-novae and cosmic rays," *Phys. Rev.*, vol. 46, pp. 76–77, Jul 1934.

[2] J. Morrison, *Modern physics: for scientists and engineers.* Academic Press, 2015.

[3] D. Fehling, "The standard model of particle physics: A lunchbox's guide,"

[4] D. Nadyozhin, "Gamow and the physics and evolution of stars," *Space Science Reviews*, vol. 74, no. 3-4, pp. 455–461, 1995.

[5] E. Witten, "Cosmic separation of phases," *Phys. Rev. D*, vol. 30, pp. 272–284, July 1984.

[6] P. Bhattacharjee, "Do 'quark-stars' exist?," *Fortschr. Phys.*, vol. 34, pp. 817–827, 1987.

[7] B. R. Martin, *Nuclear and particle physics: an introduction.* John Wiley & Sons, 2006.

[8] M. Alonso and E. J. Finn, "Fundamental university physics, vol. iii," *American Journal of Physics*, vol. 37, no. 2, pp. 235–235, 1969.

[9] T. L. Wilson, K. Rohlfs, and S. Hüttemeister, *Tools of radio astronomy*, vol. 5. Springer, 2009.

[10] M. L. Kutner, *Astronomy: A physical perspective.* Cambridge University Press, 2003.

[11] S. Chandrasekhar, "On stars, their evolution and their stability," *Reviews of modern physics*, vol. 56, no. 2, p. 137, 1984.

[12] Y. Lim, C. H. Hyun, and C.-H. Lee, "Nuclear equation of state and neutron star cooling," *International Journal of Modern Physics E*, vol. 26, no. 04, p. 1750015, 2017.

[13] D. C. Giancoli, *Physics for scientists and engineers.* Pearson Education International, 2008.

[14] G. Watanabe and T. Maruyama, "Nuclear pasta in supernovae and neutron stars," *arXiv preprint arXiv:1109.3511*, 2011.

[15] F. Weber, "Strange quark matter and compact stars," *Progress in Particle and Nuclear Physics*, vol. 54, no. 1, pp. 193–288, 2005.

[16] A. Antognini, F. Nez, K. Schuhmann, F. D. Amaro, F. Biraben, J. M. R. Cardoso, D. S. Covita, A. Dax, S. Dhawan, M. Diepold, L. M. P. Fernandes, A. Giesen, A. L. Gouvea, T. Graf, T. W. Hänsch, P. Indelicato, L. Julien, C.-Y. Kao, P. Knowles, F. Kottmann, E.-O. Le Bigot, Y.-W. Liu, J. A. M. Lopes, L. Ludhova, C. M. B. Monteiro, F. Mulhauser, T. Nebel, P. Rabinowitz, J. M. F. dos Santos, L. A. Schaller, C. Schwob, D. Taqqu, J. F. C. A. Veloso, J. Vogelsang, and R. Pohl, "Proton Structure from the Measurement of 2S-2P Transition Frequencies of Muonic Hydrogen," *Science*, vol. 339, p. 417, Jan. 2013.

[17] F. Mandl, *Statistical Physics.* Wiley, 2 ed., 11 1988.

[18] A. W. Thomas and W. Weise, *The structure of the nucleon.* John Wiley & Sons, 2010.

[19] D. D. Tong, *Quantum Field Theory.* University of Cambridge, 2007.

[20] O. R. Pols, *Stellar Structure and Evolution.* Utrecht University, 2011.

[21] I. Sagert, M. Hempel, C. Greiner, and J. Schaffner-Bielich, "Compact stars for undergraduates," *European journal of physics*, vol. 27, no. 3, p. 577, 2006.

[22] J. R. Oppenheimer and G. M. Volkoff, "On Massive Neutron Cores," *Physical Review*, vol. 55, pp. 374–381, Feb. 1939.

[23] R. C. Tolman, "Static Solutions of Einstein's Field Equations for Spheres of Fluid," *Physical Review*, vol. 55, pp. 364–373, Feb. 1939.

[24] C. D. Ott, "Static spherically-symmetric stellar structure in general relativity," July 2013.

[25] G. P. Horedt, *Polytropes: applications in astrophysics and related fields*, vol. 306. Springer Science & Business Media, 2004.

[26] A. Maeder and G. Meynet, "Stellar evolution with rotation vi: the eddington and omega-limits, the rotational mass loss for ob and lbv stars," *arXiv preprint astro-ph/0006405*, 2000.

[27] J. R. Chasnov, "Introduction to numerical methods," *The Hong Kong University of Science and Technology*, 2012.

[28] P. Flores and H. Lankarani, "Formulation for planar multibody dynamics," 01 2012.

[29] R. J. Nemiroff, "Visual distortions near a neutron star and black hole," *American Journal of Physics*, vol. 61, no. 7, pp. 619–632, 1993.

[30] J. Lattimer and M. Prakash, "The physics of neutron stars," *Science*, vol. 304, no. 5670, pp. 536–542, 2004.

[31] C. F. Gauß, "Besprechung des buchs von la seeber: Untersuchungen uber die eigenschaften der positiven ternaren quadratischen formen usw," *Gottingensche Gelehrte Anzeigen*, vol. 2, pp. 188–196, 1876.

[32] C. Amsler, P. D. Group, *et al.*, "Pl b667, 1 (2008)," *Quantum numbers shown are quark.*

[33] H. F. Jones, *Groups, representations and physics.* CRC Press, 1998.

[34] K. A. Olive, P. D. Group, *et al.*, "Review of particle physics," *Chinese Physics C*, vol. 38, no. 9, p. 090001, 2014.

[35] S. Balberg, I. Lichtenstadt, and G. B. Cook, "Roles of hyperons in neutron stars," *The Astrophysical Journal Supplement Series*, vol. 121, no. 2, p. 515, 1999.

[36] R. Ouyed, J. Dey, and M. Dey, "Quark-nova," *Astronomy & Astrophysics*, vol. 390, no. 3, pp. L39–L42, 2002.

[37] B. P. Abbott, R. Abbott, T. Abbott, F. Acernese, K. Ackley, C. Adams, T. Adams, P. Addesso, R. Adhikari, V. Adya, *et al.*, "Gw170817: observation of gravitational waves from a binary neutron star inspiral," *Physical Review Letters*, vol. 119, no. 16, p. 161101, 2017.

[38] M. Mannarelli and F. Tonelli, "Gravitational wave echoes from strange stars," *arXiv preprint arXiv:1805.02278*, 2018.

[39] I. I. Shapiro, "Fourth Test of General Relativity," *Physical Review Letters*, vol. 13, pp. 789–791, Dec. 1964.

Appendices

A Solving the Tolmann-Oppenheimer-Volkoff Equations

A.1 Integrating the differential equations

The script below integrates the relativistic equation of mass conservation and hydrostatic equilibrium iteratively using the Range-Kutta 4th order method.

```
#!/usr/bin/env python
# Author: Leander van Beek
# Dependencies: Numpy, Matplotlib, Python2.3
# Description: Solves the TOV-equations for a polytropic equation of state.
#   The polytropic eos can have arbitrary constants set.
#   The ode's are solved by a RK4O-integrator

from __future__ import print_function, division
import numpy as np
import matplotlib
matplotlib.use('agg')
import matplotlib.pyplot as plt
import time

#####################################
# Defining constants        #
#####################################

G = 6.674 * 10**(-8) #dyne cm^2/g^2
c = 29979200000 #cm/s

#####################################
# Defining functions        #
#####################################

def RK4(x_0, x_f, delta_x, y_0, deriv, *add_param):
  """
  Function RK4
  Solves ODE's numerically according to Runge-Kutta's 4th order method

  x_0 (float):    Start of solving interval
  x_f (float):    End of solving interval
  delta_x (float):  timestep over x
  y_0 (float):    Initial condition y(x=0)
  deriv (func):   Function that describes the ode
  """

  k1 = deriv(x_0, y_0, *add_param)
  k2 = deriv(x_0 + delta_x/2, y_0 + k1*delta_x/2, *add_param)
  k3 = deriv(x_0 + delta_x/2, y_0 + k2*delta_x/2, *add_param)
  k4 = deriv(x_0 + delta_x, y_0 + k3*delta_x, *add_param)

  f_estimate = y_0 + delta_x*(k1/6 + k2/3 + k3/3 + k4/6)

  return f_estimate


def rho(p, K, gamma):
  rho_l = (p/K)**(1/gamma)
  return rho_l

def epsilon(p, K, gamma):
  rho_l = rho(p, K, gamma)
  epsilon_l = p/((gamma - 1)*rho_l)
```

```
    return epsilon_l

def dpdr(p, m, r, K, gamma):
    rho_l = rho(p, K, gamma)
    epsilon_l = epsilon(p, gamma, rho_l)
    dpdr = -(rho_l*(1+epsilon_l)+p)*((m+4*np.pi*r**3*p)/(r*(r-2*m)))
    return dpdr

def dmdr(p, r, K, gamma):
    rho_l = rho(p, K, gamma)
    epsilon_l = epsilon(p, gamma, rho_l)
    dmdr = 4*np.pi*r**2*rho_l*(1+epsilon_l)
    return dmdr

#def dpdr_cgs(p, m, r, K, gamma):
def dpdr_cgs(r, p, m, K, gamma):
    rho_l = rho(p, K, gamma)
    epsilon_l = epsilon(p, gamma, rho_l)
    dpdr = -G*(rho_l*(1+epsilon_l/(c**2))+p/(c**2))*((m + 4*np.pi*r**3*p/(c**2))/(r*(r-2*G*m/(c**2))))
    return dpdr

#def dmdr_cgs(p, r, K, gamma):
def dmdr_cgs(r, m, p, K, gamma):

    #p, K, gamma = attrib # unfortunately, additional parameters are passed like this since
                # the integrator does not know how many optional arguments it gets

    rho_l = rho(p, K, gamma)
    epsilon_l = epsilon(p, gamma, rho_l)
    dmdr = 4*np.pi*r**2*rho_l*(1+epsilon_l/c**2)
    return dmdr

#####################################
#     Ask and process user input    #
#####################################

print("Welcome to this TOV-integrator!")
print("This script makes use of the Range-Kutta 4th order method. \n")

p0 = input("What is the central pressure of the star (default is 5*10^34 dyne/cm^2)? ")
gamma = input("What is the polytropic exponent gamma = (n+1)/n (default is 2.75)? ")
K = input("What is the proportionality constant (default is 1.98183*10^-6)? \n")

if p0 == "":
    p0 = np.array([5*10**(34)])
elif p0 == "array":
    p0 = 10**np.linspace(30, 50, 100) #dyne/cm^2
else:
    p0 = np.array([eval(p0)])

if gamma == "":
    gamma = 2.75
else:
    gamma = eval(gamma)

if K == "":
    K = 1.98183*10**(-6)
```

```
else:
  K = eval(K)

#print("The constants have been set! \n p0 = {0:+e} \n gamma = {1} \n K = {2:+e} \n".format(p0, gamma, K))

#####################################
#   Setup integration intervals   #
#####################################

max_km_1 = 13
max_km_2 = 15
max_km_3 = 21
r = np.linspace(0, np.log10(max_km_1*10**3*10**2), 10**4)
r = 10**r
r_2 = np.linspace(max_km_1*10**5, max_km_2*10**5, 10**4)
r_2 = np.log10(r_2)/np.log10(20)
r_3 = np.linspace(max_km_2*10**5, max_km_3*10**5, 10**4)
r_3 = np.log10(r_3)/np.log10(40)
r = np.concatenate([r, 20**r_2, 40**r_3])
m = np.zeros(len(r))
p = np.zeros(len(r))
print(len(r))

f = open("tovOutput/M-R.dat", "w+")
f.write("M R P0\n")

for j in range(len(p0)):

  f2 = open("tovOutput/pressureProfile{0}.dat".format(j), "w+")
  f2.write("# Pressure profile for a neutron star with K = {0} gamma = {1}\n".format(K, gamma))
  f2.write("Radius Density\n")
  #####################################
  #   Start integration procedure   #
  #####################################

  t_start = time.time() # measure the time for the integration process

  # The first steps have to be made manually, because there is a singularity for r=0
  p[0] = p0[j] # Set the initial condition P(r=0) = p0
  m[0] = 0 # Set the initial condition m(r=0) = 0
  delta_r = r[1] - r[0]
  m[1] = dmdr_cgs(r[1], m[0], p[0], K, gamma)*delta_r # Make the first step by Euler's approximation
  p[1] = p[0] + dpdr_cgs(r[1], p[0], m[0], K, gamma)*delta_r

  fail_i = 0
  print("The integration process has started!")
  for i in range(len(p))[2:]:
    percentage = i/len(p)*100
    print("{0:.2f}% of the total, radius now is {1:.2f} km.".format(percentage, r[i]/(10**5)))
    delta_r = r[i] - r[i-1]
    m[i] = RK4(r[i-1], r[i], delta_r, m[i-1], dmdr_cgs, p[i-1], K, gamma)
    p[i] = RK4(r[i-1], r[i], delta_r, p[i-1], dpdr_cgs, m[i-1], K, gamma)

    f2.write("{0} {1}\n".format(r[i], rho(p[i], K, gamma)))

    if np.isnan(p[i]) == True:
      fail_i = i
      break;
```

```
    t_finish = time.time();
    delta_t = t_finish - t_start

    f2.close()

    print("For index i = ", fail_i , " we have p_final/p_0 = ", (p[fail_i -1]/
      p0[j]), ". Integration stops.")

    print("Done! Total integration time: {0:.2f} s".format(delta_t))

    ####################################
    # Configure the plotting           #
    ####################################

    p_rel = p/p0[j]

    fig = plt.figure()
    fig.suptitle("M and R for $P_0 = {0:.2E}$ dyne/cm^2, $K = {1:.3E}$, $\
      gamma = {2}$".format(p0[j], K, gamma))

    fig.subplots_adjust(wspace=0.4)
    frame1 = fig.add_subplot(1,2,1)
    frame1.plot(r[:fail_i]/np.max(r[:fail_i]), p_rel[:fail_i])
    frame1.set_title(r"Pressure P(r), R={0:.2f} km".format(r[fail_i]/(10**5)))
    frame1.set_xlabel(r"Radius ($r/R_0$)")
    frame1.set_ylabel(r"Pressure $P(R)/P_0$")
# frame1.set_xlim(0, 18)

    frame2 = fig.add_subplot(1,2,2)
    frame2.plot(r[:fail_i]/np.max(r[fail_i]), (m[:fail_i]/(2*10**33)))
    frame2.set_title(r"Mass M(r), $M(R)={0:.2f} M_{{\odot}}$".format(m[fail_i
      ]/(2*10**33)))
    frame2.set_xlabel(r"Radius ($r/R_0$)")
    frame2.set_ylabel(r"M ($M_{\odot}$)")
    plt.savefig("tovOutput/{0}.png".format(j), bbox_inches="tight")

    f.write("{0} {1} {2}\n".format(m[fail_i]/(2*10**33), r[fail_i]/(10**5), p0
      [j]))

f.close()

exit()
```

scripts/solveTOV.py

A.2 Making an M-R plot of the results of the TOV-equations

The results of several central densities have been used to generate masses and radii for sample stars in the last script. This script plots those results from the exported .dat file using matplotlib.

```
#!/usr/bin/env python
# Author: Leander van beek

from __future__ import print_function, division

import numpy as np
import matplotlib
matplotlib.use('agg')
import matplotlib.pyplot as plt

```

```
def M_s(R):
    """
    IMPORTANT
    This function is designed to return the Schwarzschild mass in solar
    masses for a radius in kilometers. It's a quick and dirty plot and is
    not flexible in any way.
    """

    M_s = R/2.97
    return M_s

M, R, P0 = np.loadtxt("tovOutput/M-R.dat", skiprows=1, unpack=True)

r = np.linspace(8, 15, 100)
M_schwarzschild = M_s(r)

fig = plt.figure()

frame = fig.add_subplot(1,1,1)
frame.set_title("M-R plot for Neutron stars")
frame.set_xlabel("Radius (km)")
frame.set_ylabel("Mass (solar)")
plt.grid()
frame.plot(R, M)
#frame.plot(r, M_schwarzschild)
plt.savefig("tovOutput/MRPlot.png")
```

scripts/plotMR.py

A.3 Determining the binding energies and baryon numbers

A configuration of a neutron star is picked from the generated dataset. From this configuration, the pressure-radius-density profile is retrieved, after which the baryon numbers and binding energies are computed for all shells.

```
#!/usr/bin/env python

from __future__ import print_function, division
import numpy as np
import matplotlib.pyplot as plt
import time
from matplotlib import rc

r, rho = np.loadtxt('tovOutput/pressureProfile0.dat', comments="#", unpack=
    True, delimiter=" ", skiprows=2)
r = r[:-1]/(10**2)
rho = rho[:-1]*(10**3)
c = 299792458 # m/s
G = 6.674 * 10**(-11) #N m^2/kg^2
M_grav = np.zeros(len(r))
M_bind = np.zeros(len(r))
m_b = 1.672*10**(-27) # kg
N = np.zeros(len(r))
N[0] = 1

for i in range(len(r))[1:]:
    delta_r = r[i]-r[i-1]
    M_grav[i] = M_grav[i-1] + 4*np.pi*r[i]**2*delta_r*rho[i]

    N[i] = M_grav[i]/(m_b*(1-G*M_grav[i]/r[i]/c**2))

    delta_N = N[i] - N[i-1]
```

```
    M_bind[i] = M_bind[i-1] - delta_N*m_b*G*M_grav[i]/r[i]/(c**2)

M_bar = m_b * N

fig = plt.figure()
frame = fig.add_subplot(2, 2, 1)
frame2 = fig.add_subplot(2, 2, 2)
frame3 = fig.add_subplot(2, 2, 3)
frame4 = fig.add_subplot(2, 2, 4)
frame.plot(r/10**3, M_grav/(2*10**30), label="Gravitational")
frame.plot(r/10**3, M_bar/(2*10**30), label="Baryonic")
frame2.plot(r/10**3, M_bind/(2*10**30), label="Equation")
frame2.plot(r/10**3, M_grav-M_bar, label="Difference plot 1")
frame3.plot(r/10**3, np.log10(N))
frame4.plot(np.log10(N), M_bind*c**2/N*(6.242*10**(12)), label="BE")

frame.set_title("Mass")
frame.set_ylabel("M ($M_{\odot}$)")
frame.set_xlabel("r (km)")
frame.legend(loc="best")

frame2.set_title("Binding mass")
frame2.set_xlabel("r (km)")
frame2.set_ylabel(r"Binding energy/$c^2$ ($M_{\odot}$)")
frame2.legend(loc="best")


frame3.set_title("Baryon Number")
frame3.set_xlabel("r (km)")
frame3.set_ylabel("$\log_{10}$ Baryon number")

frame4.set_title("BE per baryon")
frame4.set_xlabel("$\log_{10}$ Baryon number")
frame4.set_ylabel("Binding Energy (MeV)")
frame4.set_ylim([-100, 10])
#frame4.set_ylim([-1200, 100])
#frame4.axhline(y=-1115.683, color="r", label=r"$\Lambda$")
frame4.legend(loc="best")

plt.show()
```

scripts/massPerBaryon.py